



Discovery of 2-(cyclopropanecarboxamido)-N-(5-((1-(4-fluorobenzyl)piperidin-4-yl)methoxy)pyridin-3-yl)isonicotinamide as a potent dual AChE/GSK3 β inhibitor for the treatment of Alzheimer's disease: Significantly increasing the level of acetylcholine in the brain without affecting that in intestine



Xueyang Jiang^a, Chang Liu^c, Manxing Zou^a, Huanfang Xie^b, Tailiang Lin^e, Weiping Lyu^c, Jian Xu^a, Yuan Li^d, Feng Feng^{a, d, ***}, Haopeng Sun^{b, **}, Wenyuan Liu^{c, *}

^a Department of Natural Medicinal Chemistry, China Pharmaceutical University, Nanjing, 211198, China

^b Department of Medicinal Chemistry, China Pharmaceutical University, Nanjing, 211198, China

^c Department of Pharmaceutical Analysis, Key Laboratory of Drug Quality Control and Pharmacovigilance, China Pharmaceutical University, Nanjing, 211198, China

^d Jiangsu Food and Pharmaceutical Science College, Huai'an, 223003, China

^e College of Life Science and Technology, China Pharmaceutical University, Nanjing, 211198, China

ARTICLE INFO

Article history:

Received 8 May 2021

Received in revised form

15 June 2021

Accepted 18 June 2021

Available online 22 June 2021

Keywords:

AChE

GSK3 β

Acetylcholine

Neuroprotection

Alzheimer's disease

ABSTRACT

Acetylcholinesterase (AChE) inhibitors are currently the first-line drugs approved by the FDA for the treatment of Alzheimer's disease (AD). However, a short effective-window limits their therapeutic benefits. Clinical studies have confirmed that the combination of AChE inhibitors and neuroprotective agents exhibits better anti-AD effects. We have previously reported that the dual AChE/GSK3 β (Glycogen synthase kinase 3 β) modulators have both neuroprotective effects and cognitive impairment-improvement effects. In this study, we characterized a new backbone of the AChE/GSK3 β inhibitor **11c**. It was identified as a highly potent AChE inhibitor and was found superior to donepezil, the first-line drug for the treatment of AD. *In vivo* studies confirmed that **11c** significantly inhibited the activity of AChE in the brain but had little effect on the activity of AChE in the intestine. This advantage of **11c** was expected to reduce the peripheral side effects caused by donepezil. Furthermore, biomarker studies have shown that **11c** also improved the levels of acetylcholine and synaptophysin in the brain and exhibited neuroprotective effects. Preliminary *in vivo* and *in vitro* research results underline the exciting potential of compound **11c** in the treatment of AD.

© 2021 Elsevier Masson SAS. All rights reserved.

1. Introduction

Alzheimer's disease (AD) is an insidious, progressive, neurodegenerative syndrome, which is characterized by severe memory loss and cognitive impairment. The histopathological features of AD are mainly the neuroinflammatory amyloid plaques and

neurofibrillary tangles (NFTs) induced by the phosphorylated tau protein [1,2].

The drugs approved by the FDA for the treatment of AD are mainly acetylcholinesterase (AChE) inhibitors (donepezil, galantamine and rivastigmine) that improve the level of acetylcholine (ACh) in the brain and strengthen the synaptic transmission. The loss of cholinergic neurons and depletion of the brain neurotransmitter ACh are the main characteristics of AD. Autopsy analysis of AD patients revealed severe damage and abnormality of the basal ganglia cholinergic system [3]. The central cholinergic neurotransmitter ACh is essential for maintaining normal learning and memory in mammals [4]. Neuroscience studies have found that when the body needs to analyze and remember new stimuli in

* Corresponding author.

** Corresponding author.

*** Corresponding author. Jiangsu Food and Pharmaceutical Science College, Huai'an, 223003, China.

E-mail addresses: fengfeng@cpu.edu.cn (F. Feng), sunhaopeng@163.com (H. Sun), liuwenyuan8506@163.com (W. Liu).

cognitive activities, cholinergic neurons in the basal forebrain are activated, and the release of ACh in the brain is increased [5]. The level of acetylcholinesterase (AChE) in the hippocampus and cortex of AD patients is higher; it can hydrolyze ACh and reduce the synaptic concentration lower than the normal [6]. Therefore, improving the level of ACh by inhibiting AChE is an important method to improve the cognitive impairment of AD patients [7]. The selective AChE inhibitor donepezil is the only first-line drug approved by the FDA and MCA for the treatment of mild-to-moderate AD [8].

The synthesis of the ACh neurotransmitter from choline and acetyl CoA is catalyzed by the choline acetyltransferase; it is then stored in the synaptic vesicles. The progression of AD results in the degeneration of the cortex, atrophy of the hippocampus, and neuroinflammation that consequently lead to the disappearance of the cholinergic neurons and synapses [9]. This is the reason for the deteriorating effect of AChE inhibitors in the middle and later stages of AD. Interestingly, AChE inhibitors combined with neuroprotective agents produced better anti-AD effects [10]. Memantine is a non-competitive, *N*-methyl-*D*-aspartate receptor (NMDA) antagonist with medium affinity. It might protect neurons from NMDA receptor-mediated degeneration [11,12]. The combination therapy of donepezil and memantine (Namzaric®) was approved in 2014 for the treatment of moderate-to-severe AD patients [13]. Compared with the administration of AChE inhibitors alone, the combination therapy reduced the severity of the neurobehavioral symptoms, reduced the rate of cognitive decline, and delayed admission to nursing homes [14]. However, the co-administration of two or more drugs may lead to undesirable pharmacokinetic changes and increase toxic side effects, thus limiting the application of combination therapy [15].

Glycogen synthase kinase 3 β (GSK3 β) is highly expressed in neurons and astrocytes and plays an important role in the development of AD [16]. The first step may involve the hyperactivation of the GSK3 β in the brain of AD patients. It causes the hyperphosphorylation of the tau protein, and subsequently, a decrease in the affinity of tau and microtubule [17]. Hyperphosphorylated tau leads to microtubule disassembly and NFT formation. This contribution confers tau a key role in the pathogenesis of AD. Secondly, over-activated GSK3 β can cause astrocyte axon contraction and synapse damage [18]. Additionally, it can promote the activation of the microglia and the expression of pro-inflammatory factors, thereby exacerbating neuronal damage. As expected, GSK3 β inhibitors can decrease the inflammatory response of astrocytes and microglia in the central nervous system and thereby reduce the apoptosis of the nerve cells [19–21]. Our previous work based on the proteolysis targeting chimeras (PROTACs) strategy reported that the first GSK3 β protein degradation agent also showed neuroprotective effects [22]. Importantly, long-term use of the GSK3 β inhibitor lithium chloride significantly reduced the level of phosphorylated tau in the cerebrospinal fluid in AD patients and successfully alleviated the decline in the cognitive ability of the patients without significant side effects [23].

Considering the above statements, it was believed that AChE/GSK3 β dual inhibitors may not only increase the level of ACh in the brain but also reduce the phosphorylation of tau and protect neurons. These actions may overcome the drawback of the short therapeutic window generated by the use of AChE inhibitors alone. Oukoloff et al. developed a series of AChE/GSK3 β inhibitor (**1**) based on tacrine and valmerin fragments using copper (I)-catalyzed azide-alkyne cycloaddition (CuAAC) [24]. Likewise, Xu et al. patented a series of AChE/GSK3 β inhibitor (**2**) based on tacrine and pyrimidinone fragments (Fig. 1) [25]. Two series of AChE/GSK3 β inhibitors (**3**, **4**) were designed based on the AChE inhibitor tacrine using a splicing strategy in our previous work [26,27]. However, the

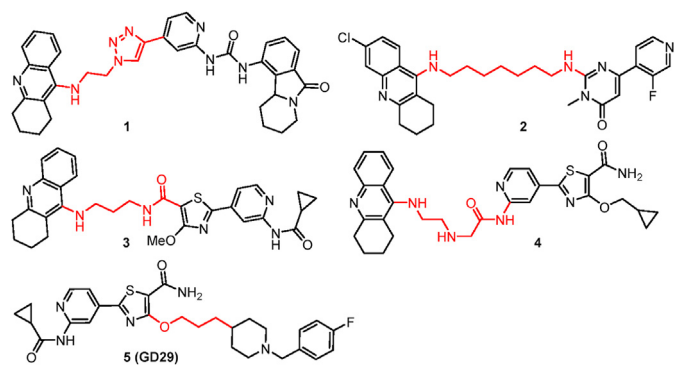


Fig. 1. Structures of dual AChE/GSK3 β inhibitors.

flexible linker and the urea functionality of the compound were potential drawbacks in terms of metabolic stability. The co-crystal structure of the di-tacrine dimer and donepezil and AChE indicated that the benzylpiperidine part of donepezil overlapped with the tacrine fragment and formed a π - π stacking interaction with the Trp 84 residue of the catalytically active site (CAS) (Fig. S1 in Supporting Information). Subsequently, the tacrine fragment was replaced with a benzyl piperidine group, and the fused compound **5** (GD29) was obtained [28]. GD29 displayed permeability of and safety in the hemorrhage-brain barrier but poor AChE inhibitory activity, which may be caused by the steric hindrance of formamide (Fig. 2A).

Herein, our findings on the chemical optimization and pharmacological evaluation of novel AChE/GSK3 β inhibitors are disclosed. The methodology was based on fusion strategy and incorporated the pharmacophore of donepezil (**7**) and GSK3 β inhibitors (**6**, **8**). A series of novel *N*-(5-(piperidin-4-ylmethoxy)pyridin-3-yl)isonicotinamide analogs have been identified as potent AChE/GSK3 β inhibitors with potency in the nanomolar range and varying levels of improved efficacy. This work culminated in the discovery of compound **11c** (structure in Fig. 4) that was found to be an orally bioavailable, brain-penetrant, and potent AChE/GSK3 β inhibitor. This novel inhibitor exhibited improvement in the level of acetylcholine and cognitive impairment, thus suggesting a therapeutic potential for Alzheimer's disease.

2. Results and discussion

Design of novel AChE/GSK3 β inhibitors. The previously reported AChE/GSK3 β inhibitors based on the splicing strategy contained a flexible linker and tacrine moiety. These two molecules had potential drawbacks in terms of metabolic stability and safety and this limited their use as pharmacological tools or potential drug candidates. The X-ray co-crystal structure of donepezil in the human AChE displayed a deep and narrow active site gorge consisting of two separated ligand-binding sites: the peripheral anionic binding site (PAS) and the catalytic active site (CAS). The PAS is located close to the mouth of the active site gorge with an aromatic residue Trp286 as the important anionic site. The CAS contains the AChE catalytic triad (Ser 203/Glu 334/His 447) and the important aromatic residue Trp86 at the bottom of the gorge. The benzyl piperidine group of donepezil was localized at the entrance of the gorge and on the PAS, and the indanone ring was stacked against the Trp 286 residue forming a π - π stacking interaction. The piperidine group extended to the bottom of the gorge and formed a π - π interaction with Trp86 residue (Fig. S2 in Supporting Information). This phenomenon meant that the benzyl piperidine group was the key group that enabled donepezil to execute the AChE

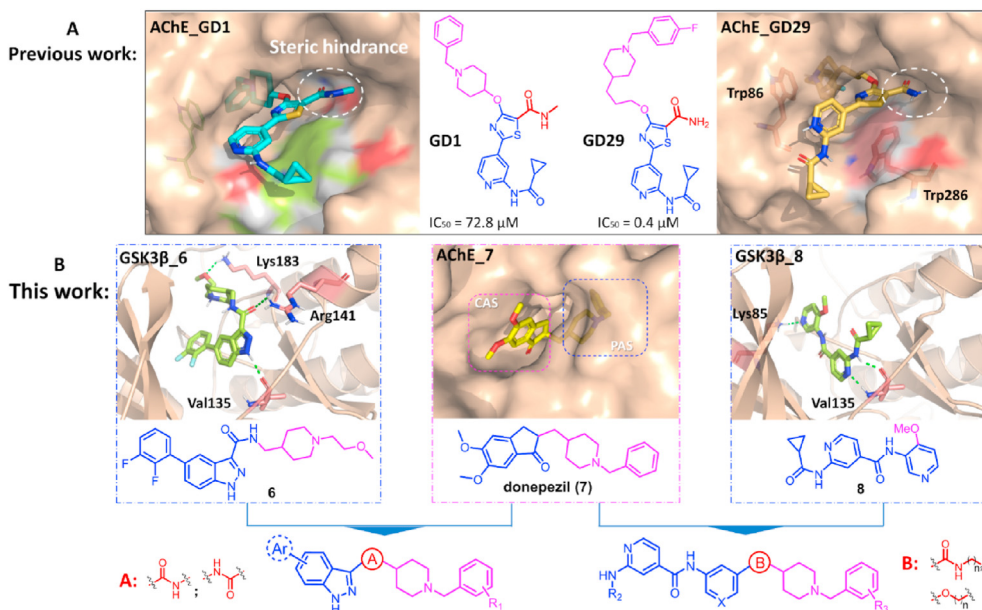


Fig. 2. Design of the merged dual AChE/GSK3 β inhibitors. The design of AChE/GSK3 β inhibitors (**GD1** and **GD29**) based on acylaminopyridine fragments in our previous work. In the presented work, we designed a dual AChE/GSK3 β inhibitor based on benzopyrazole and isonicotinamide fragments.

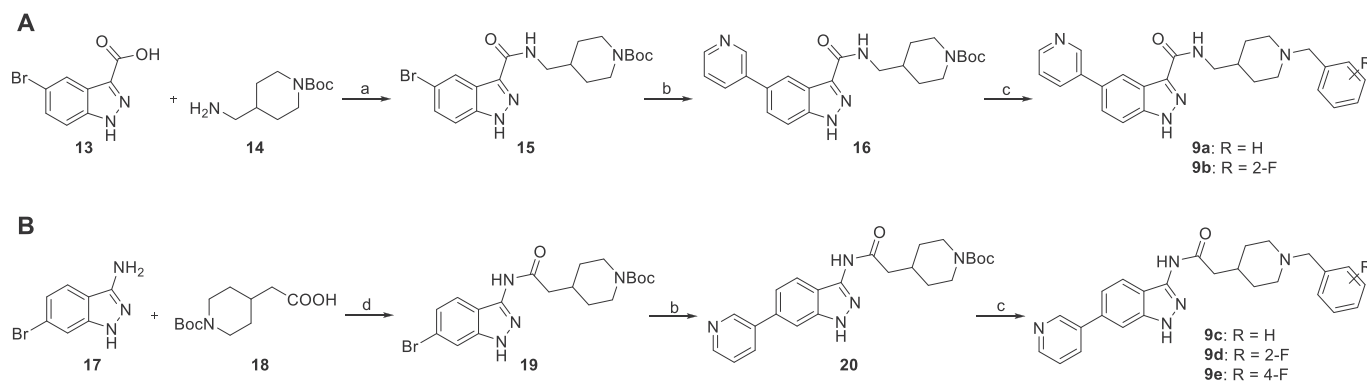
inhibitory activity. Therefore, we employed the pharmacophore fusion design strategy: the benzyl-piperidine of the AChE inhibitor was used as the essential pharmacophore and was fused with the indazolyl-carboxamide pharmacophore of the GSK3 inhibitor (**6**) [29] and pyridyl-isonicotinamide of the GSK3 inhibitor (**8**) [30], respectively. The fused compounds were used as the starting points for exploration of the structure-activity relationship (SAR) (Fig. 2B).

Synthesis. Synthetic route of benzopyrazole compounds **9a–9d** is schematically illustrated in Scheme 1. 5-Bromobenzopyrazole-3-carboxylic acid (**13**) was condensed under dicyclohexylcarbodiimide (DCC) conditions with 1-boc-4-aminomethylpiperidine (**14**) to give intermediate **15**, which then was allowed to undergo Suzuki-Miyaura coupling reaction with 3-pyridylboronic acid to form intermediate **16**. The Boc protecting group of **16** were hydrolyzed with trifluoroacetic acid (TFA) and then reacted with the corresponding benzyl bromides to give the final products **9a** and **9b**. Moreover, a similar condensation of 3-amino-5-bromoindazole (**17**) was performed with 1-boc-4-piperidylacetic acid (**18**) to generate **19**, following coupling reaction with 3-pyridylboronic acid to obtain **20**. After that, compound **20** were

hydrolyzed and then reacted with the corresponding benzyl bromides to generate the corresponding final products **9c–9e**.

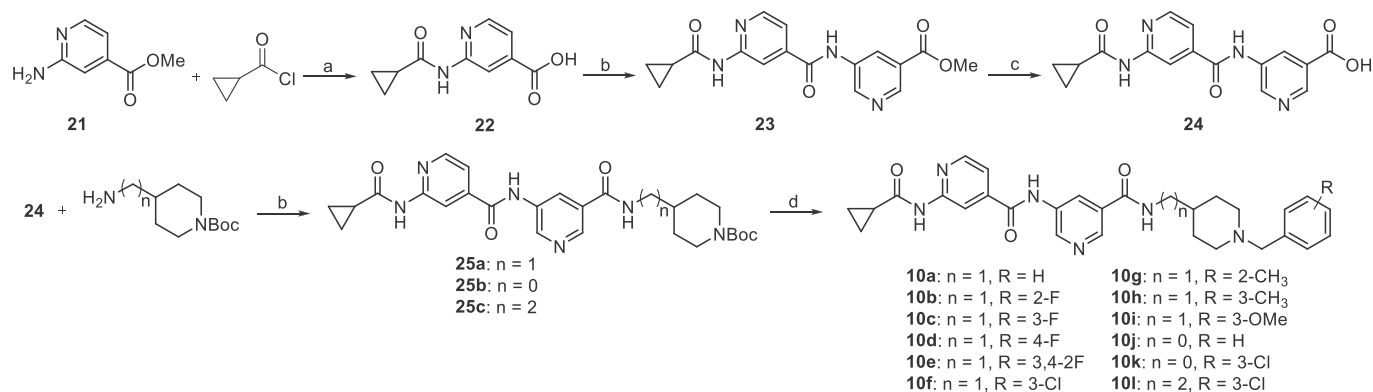
The preparation of isoniazid compounds **10a–10l** is illustrated in Scheme 2. The starting methyl 2-aminoisonicotinate (**21**) was amidated with cyclopropanecarbonyl chloride under alkaline conditions, followed by hydrolysis in the presence of LiOH to yield intermediate **22**. The condensation reaction of **22** with methyl 5-aminonicotinate under HATU conditions resulted in compound **23**, which was then hydrolyzed to give intermediate **24**. Subsequently, the corresponding diamines were attached to **24** under HATU conditions to form intermediates **25a–25c**, which were hydrolyzed and then reacted with the corresponding benzyl bromides to yield final products **10a–10l**.

The designed isoniazid compounds **11a–11j** were prepared using a palladium (0)-catalyzed Buchward coupling reaction as the key step (Scheme 3). First, phenols (**26a** and **26b**) were reacted with brominated alkanes (**27a** and **27b**) to give the aromatic bromine intermediates **28a–28c**, respectively. Second, one pot amidation and ester hydrolysis of methyl 2-aminoisonicotinate (**21**) delivered intermediates **22** and **22a**, which were readily coupled with



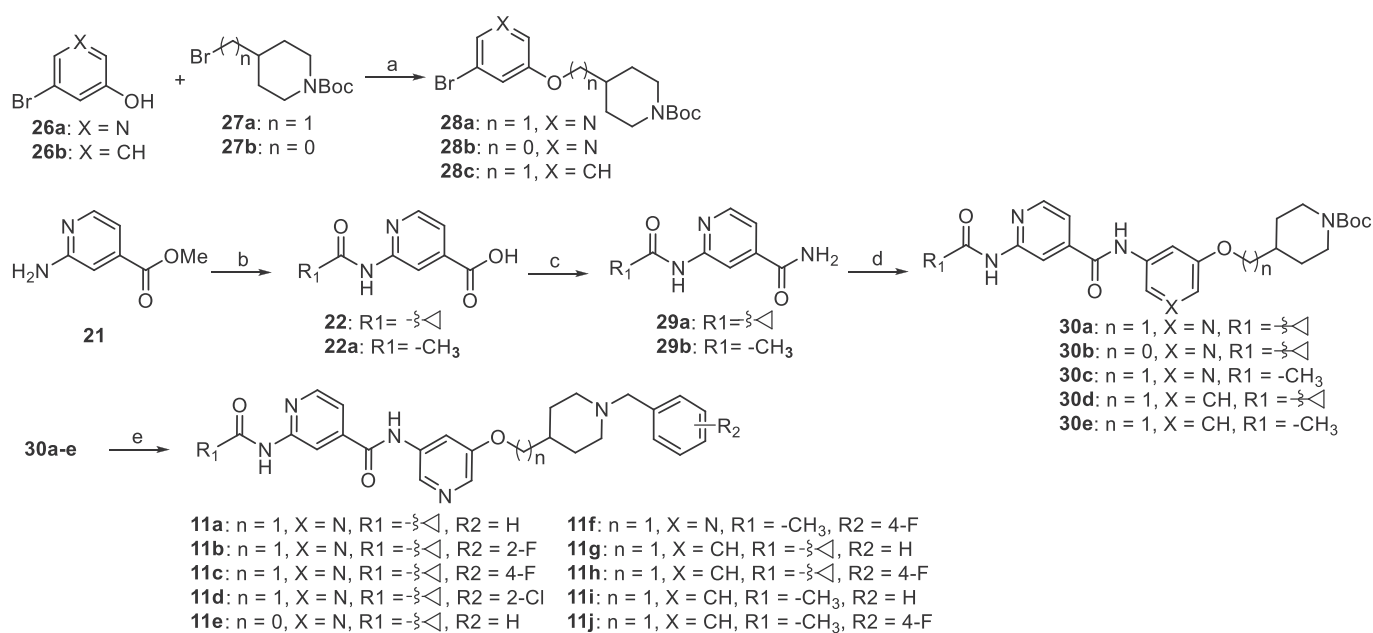
Scheme 1. Synthesis of compounds **9a–9e**^a

^aReagents and conditions: (a) DCC, HOBT, DMF, rt, 24 h; (b) 3-pyridylboronic acid, Pd (dppf)Cl₂, Cs₂CO₃, 1,4-dioxane/H₂O (3:1), 115 °C, 24 h; (c) i: TFA, DCM, rt, 3 h; ii: benzyl bromides, K₂CO₃, DMF, 55 °C, 5 h; (d) PyBOP, HOBT, DIPEA, THF, rt, 12 h.



Scheme 2. Synthesis of compounds 10a–10l^a

^aReagents and conditions: (a) i: K_2CO_3 , THF, rt, 24 h; ii: 1 N LiOH, MeOH/THF, rt, 6 h; (b) 5-aminopyridine-3-carboxylic acid methyl ester, HATU, DIPEA, DMF, rt, 24 h; (c) 1 N NaOH, MeOH/THF, rt, 7 h; (d) i: TFA, DCM, rt, 3 h; ii: benzyl bromides, K_2CO_3 , DMF, 55 °C, 5 h.



Scheme 3. Synthesis of compounds 11a–11j^a

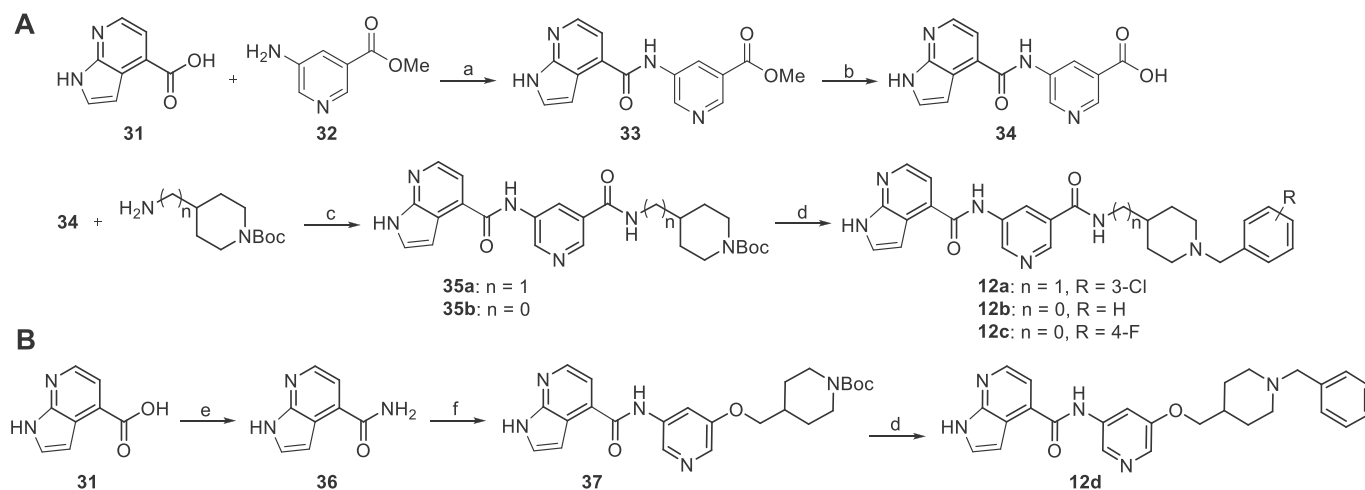
^aReagents and conditions: (a) K_2CO_3 , DMF, 60 °C, 10 h; (b) i: K_2CO_3 , THF, rt, 24 h; ii: 1 N LiOH, MeOH/THF, rt, 6 h; (c) NH_4Cl , HATU, DIPEA, DMF, rt, 36 h; (d) **28a–c**, $Pd_2(dba)_3$, xantphos, Cs_2CO_3 , 1,4-dioxane, 110 °C, 22 h; (e) i: TFA, DCM, rt, 3 h; ii: benzyl bromides, K_2CO_3 , DMF, 55 °C, 5 h.

ammonium chloride under HATU conditions to form **29** and **29a**, respectively. Further, compounds **29** and **29a** were converted to the key intermediate **30a–30e** with bromine intermediates **28a–28c** via a Buchward coupling reaction. Finally, the Boc protecting groups of **30a–30e** were removed, and then reacted with the corresponding benzyl bromides to give the final products **11a–11j**.

The synthetic procedure for compounds **12a–12d** is briefly described in Scheme 4. The preparation of compounds **12a–12c** is similar to that of compound **10**. The starting material 7-azaindole-4-carboxylic acid (**31**) reacted with methyl 5-aminonicotinate to afford compound **33**, which was then hydrolyzed to give intermediate **34**. The condensation of the carboxylic acid group of compound **34** with 1-boc-4-aminomethylpiperidine and 4-amino-1-boc-piperidine afforded compounds **35a** and **35b**. Finally, the Boc protecting groups of **35a** and **35b** were removed, and then reacted with the corresponding benzyl bromides to give the final products **12a–12c** (Scheme 4A). The condensation of 7-azaindole-4-carboxylic acid (**31**) afforded compound **36**, which readily reacted

with the aromatic bromine intermediate **28a** under Buchward coupling conditions to afford the compound **37**. Finally, the Boc protecting group of **37** was removed, and then reacted with benzyl bromide to give the final product **12d** (Scheme 4B).

In vitro evaluation of the AChE and GSK3 β inhibitory activities. The inhibitory potency on both targets was evaluated using enzyme activity assays with recombinantly expressed proteins. The enzymatic activity of AChE was performed following the method of Ellman et al. using the artificial substrate acetylthiocholine iodide [31]. The GSK3 β activity was assessed using a Kinase-Glo luminescent assay developed by Baki et al. [32] First, the ethyl methyl ether fragment in compound **6** (GSK3 β inhibitor) was replaced with a benzyl group to mimic the benzyl piperidine fragment of donepezil (Scheme 1). The replacement of the phenyl group with the pyridyl ring could improve its physicochemical properties and ensure better *in vivo* pharmacokinetic (PK) properties [33]. Additionally, the *N* atom of the pyridyl ring had an extra unshared electron pair, which could form hydrogen bonds to potentially



Scheme 4. Synthesis of compounds 12a–12d^a

^aReagents and conditions: (a) HATU, DIPEA, DMF, rt, 24 h; (b) 1 N NaOH, MeOH/THF, rt, 7 h; (c) PyBOP, HOBT, DIPEA, THF, rt, 24 h; (d) i: TFA, DCM, rt, 3 h; ii: benzyl bromides, K₂CO₃, DMF, 55 °C, 5 h; (e) NH₄Cl, HATU, DIPEA, DMF, rt, 36 h; (f) **28a**, Pd₂(dbc)₃, xantphos, Cs₂CO₃, 1,4-dioxane, 110 °C, 22 h.

improve the binding affinity. The Lys85 side chain of GSK3 β formed a key hydrogen bond with ligand acceptor groups in most inhibitors [30]. Therefore, the 3,4-2F phenyl group of **6** was replaced with a pyridine group to obtain compound **9a**. The prototype inhibitor **9a** yielded promising IC₅₀ values of 0.6 μ M (*ee*AChE), 1.1 μ M (*h*AChE), and 0.1 μ M (GSK3 β). Recently, selectively fluorinating bioactive molecules have been developed into a well-established strategy for the design of new drugs because they exhibited improved physicochemical characteristics, pharmaceutical effectiveness, and pharmacokinetic profiles [34]. Based on these findings, the benzyl group was replaced with the 2-F substituted benzyl group to obtain compound **9b**. The inhibitory potency toward AChE decreased almost 1-fold along with a slightly better IC₅₀ value for GSK3 β . Considering that the catalytic cavity of AChE was straight and elongated, the pyridine group of **9a** was changed from position 4 to position 5 to obtain a straight, linear-type compound **9c**. Compared with compound **9a**, **9c** showed better AChE inhibitory activity but lost the inhibitory ability toward GSK3 β . Further introduction of a fluorine atom into the benzyl group of **9c** was not conducive to improving the inhibition against GSK3 β (Table 1). The above SAR discussion demonstrated that pyridine in the benzopyrazole compounds required a specific attachment position to execute the inhibition of GSK3 β . However, AChE inhibitors were required to have a linear structure. Thus, it was difficult to coordinate the structure of benzopyrazole compounds to display a good inhibition toward both the enzymes.

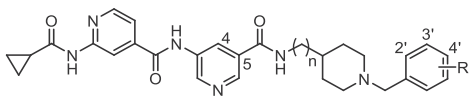
Subsequently, the attention was focused on the isonicotinamide compound **8** developed by Bristol-Myers Squibb Research & Development. It is a highly selective, brain-penetrable, and orally active GSK3 β inhibitor [30]. The X-ray structural studies depicted that the 2-aminopyridine was located in the hinge region and formed hydrogen bonds with the Val135 backbone amide. Moreover, the 3-aminopyridine sp² nitrogen formed a key hydrogen bond with the Lys85. The 4- and 5-positions of the 3-aminopyridine that faced the substrate-binding region were considered more suitable for structural modification (Fig. 2B). Considering that the AChE inhibitor was required to have a linear shape to fit the long and narrow cavity of AChE, the 5-position of pyridine in compound **8** was chosen as the structural modification site. First, a benzylpiperidine fragment was introduced at position 5 of the pyridine of compound **8** through an amide bond to obtain compound **10a** (Scheme 2). As shown in Table 2, the inhibitory activity of

Table 1
In vitro inhibitory activity of the dual AChE/GSK3 inhibitors: benzopyrazole core (9a–9e).

Compd.	R1	X	R2	IC ₅₀ (μ M)		
				<i>ee</i> AChE	<i>h</i> AChE	<i>h</i> GSK3 β
9a	4-(pyridine-3-yl)		H	0.552	1.093	0.095
9b	4-(pyridine-3-yl)		2-F	0.718	2.176	0.079
9c	5-(pyridine-3-yl)		H	0.264	0.509	>10
9d	5-(pyridine-3-yl)		2-F	0.390	0.691	>10
9e	5-(pyridine-3-yl)		4-F	0.216	0.518	>10
donepezil	–	–	–	0.021	0.044	>10
SB216763	–	–	–	n. d.	n. d.	0.029

compound **10a** on *h*AChE was similar to that of compound **9a**; the IC₅₀ value was ~ 1 μ M. Further introduction of halogen atoms such as fluorine or chlorine into the benzyl group (R position) of compound **10a** resulted in the formation of compounds **10b–10f**. However, only the 3-chloro atom-substituted compound **10f** displayed moderate inhibition against AChE with an IC₅₀ of 0.678 μ M. Subsequent addition of electron-donating groups such as 2-Me (**10g**), 3-Me (**10h**), or 3-OMe (**10i**) into the benzyl group appeared harmful for the inhibition against AChE. Different substituted benzyl groups displayed little effect on the inhibitory activity of GSK3 β ; their IC₅₀ values ranged from 0.097 to 0.305 μ M. To examine

Table 2
In vitro inhibitory activity of the dual AChE/GSK3 β inhibitors: isonicotinamide core (**10a–10l**).



Compd.	n	R	IC ₅₀ (μM)		
			eeAChE	hAChE	hGSK-3 β
10a	1	—	1.100	1.102	0.305
10b	1	2-F	1.724	1.755	0.164
10c	1	3-F	1.020	2.388	0.097
10d	1	4-F	1.156	3.029	0.244
10e	1	3,4-2 F	1.047	3.067	0.279
10f	1	3-Cl	0.678	1.091	0.231
10g	1	2-CH ₃	3.517	4.093	0.157
10h	1	3-CH ₃	4.162	6.364	0.198
10i	1	3-OMe	8.913	>10	0.126
10j	0	—	0.704	0.622	0.081
10k	0	3-Cl	0.951	2.501	0.063
10l	2	3-Cl	2.081	4.392	0.152

the influence of the length of the link between the pyridine amide group and piperidine, the methyl piperidine of compound **10f** was replaced with piperidine (**10k**) or ethyl piperidine (**10l**). Reducing or extending the length of the linking chain seemed detrimental to the inhibitory activity of AChE. It was worth noting that a reduction in the size of the link chain (**10k**) resulted in a three-fold increase in the inhibitory activity of GSK3 β relative to **10f**.

To probe the impact of the flexibility and steric availability around the linker between the pyridine group and the piperidine group, the amide bond of compound **10a** was replaced with an ether bond to obtain compound **11a** (Scheme 3). Surprisingly, the inhibitory activity of **11a** on AChE increased 500 times relative to that of **10a**, suggesting that the introduction of ether bonds reduced the steric hindrance and increased the flexibility. Thus, benzylpiperidine easily extended into the CAS of AChE. To gain insight into the above assumption, a molecular docking study was implemented using the Maestro module of Schrödinger. The docking results demonstrated that the benzyl group of **11a** formed a more stable π - π interaction with Trp86 of AChE (Fig. 3). Besides, the 2-aminopyridine fragment of compound **10a** was located in the solvent-exposed region that was similar to the **GD29**_AChE docking pattern reported in our previous report (Fig. 2A). Regarding the GSK3 β inhibitory activity, replacement of the amide bond (**10a**) with an ether bond (**11a**) caused an approximately 13-fold increase in the potency compared to **10a**. Encouraged by this result, different halogen atom substituents (e.g., **11b**, **11c**, and **11d**) were introduced

on the benzene ring (R2 position). Remarkably, when the *F* moiety was introduced in the para-position of the benzene ring (**11c**), an excellent inhibition against hAChE was observed with an IC₅₀ value of 1.0 nM (Table 3). However, when the methyl piperidine group of **11a** was replaced with a piperidine group (**11e**), the inhibitory activity of AChE decreased dramatically. To examine the influence of the steric hindrance caused by the cyclopropanoyl, an acetyl substituent (**11f**) was prepared and evaluated. Compound **11f** exhibited a slightly higher AChE inhibitory activity but resulted in an approximately 100-fold loss of potency and an IC₅₀ value of 3.5 μM relative to compound **11c**. Compounds **11g–11j** were then designed and synthesized to explore the effect of the pyridine ring on potency. The enzyme inhibitory activity results illustrated that all compounds displayed different degrees of substantial loss of potency for the two enzymes. Thus, the pyridine ring connected to the ether bond played an important role in compound potency.

To understand the potential binding mode and receptor-ligand interactions, molecular docking using Schrödinger and PyMOL 2.3 software was employed. Compound **11c** was selected as an example from among our optimized compounds to further explore the binding interactions with hAChE (PDB ID: 4ey7) and hGSK3 β (PDB ID: 4f94). The docking results indicated that compound **12c** displayed energetically favorable interactions with the narrow pocket and formed a binding pose similar to that between donepezil and AChE in the solved co-crystal structure (Fig. 4A). The fluorinated benzyl ring was stacked against Trp86 in the CAS (Fig. 4B). Further, the potent AChE inhibitory activity of **11c** may be related to these factors (Fig. 4C). First, the 2-fluoro substituent formed an important multipolar fluorine-backbone interaction with Tyr133 and Gly 120. Second, the pyridine group (A-ring) formed a π - π stacking with Trp286 and Tyr72. Third and the most important point, the pyridine group (B-ring) stacked against Trp286 and the N atom on the pyridine ring formed a critical hydrogen bond with Arg296. This orientation might explain the loss in the AChE inhibitory activity due to the replacement of pyridine with benzene ring (**11a** vs **11g**). The molecular dynamics simulation studies also validated the docking results that the residues Trp86, Trp286, and Arg296 played key roles in the protein-ligand interactions (Fig. S3 in Supporting Information). On the other hand, the docking results of compound **11c** and GSK3 β showed that the isonicotinamide fragment occupied the ATP catalytic site (Fig. 4D). Specifically, the A-ring formed a hydrogen bond with residues Tyr134 and Val135, and the B-ring formed a hydrogen bond with Lys85 (Fig. 4E). Moreover, the benzyl piperidine group occupied the substrate-binding area, and the fluorine atom of the C-ring formed a hydrogen bond with Asn 64 (Fig. 4F).

Finally, to further avoid the steric hindrance caused by the cyclopropanoyl group, *N*-(pyridin-2-yl) cyclopropanecarboxamide was replaced with 1*H*-pyrrolo [2,3-*b*] pyridine, and compounds **12a–12d** were synthesized (Scheme 4). Unfortunately, the

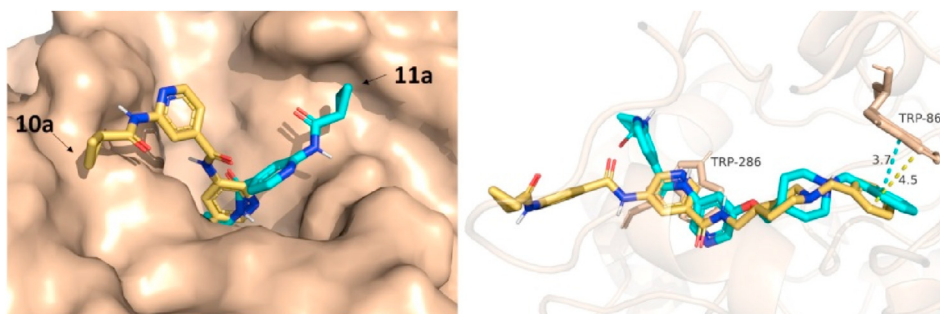


Fig. 3. Eutectic overlay of the bonding modes of compounds **10a** and **11a** with AChE (PDB id: 4ey7). The isonicotinamide fragment of **10a** was located in the solvent exposure zone of AChE.

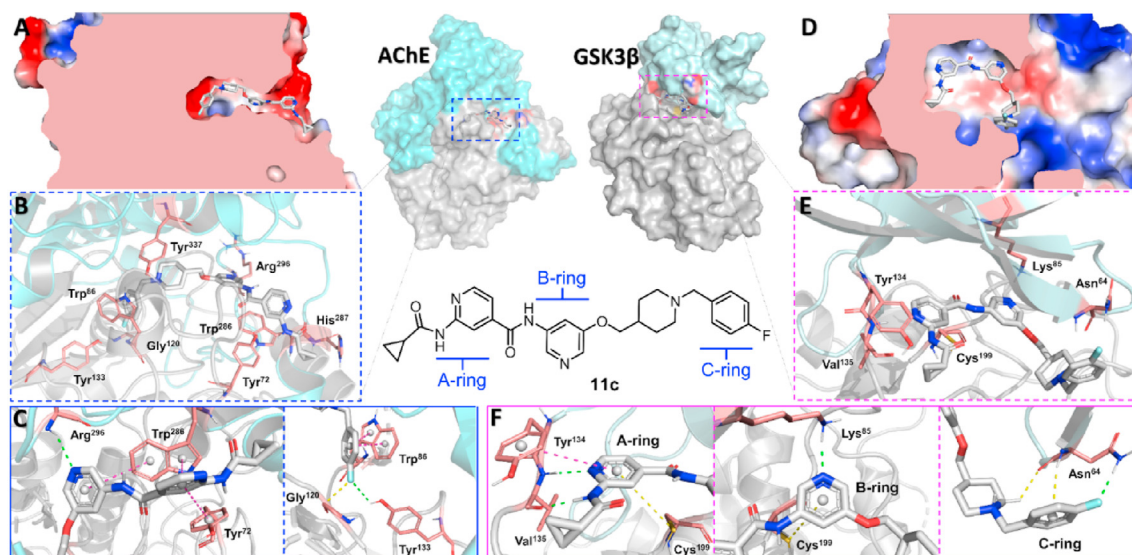
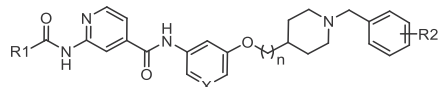


Fig. 4. Analysis of the binding modes of **11c** with AChE and GSK3 β . (A) The docking site of **11c** was derived from the position of the small molecular ligand co-crystallized in the binding sites of AChE (PDB id: 4ey7). (B) The binding modes of **11c** with AChE. (D) The docking site of **11c** was derived from the position of the small molecular ligand co-crystallized in the binding sites of GSK3 β (PDB id: 4f94). (E) The binding modes of **11c** with GSK3 β . The hydrogen bonds are shown as green dashed lines.

Table 3

Inhibition of the enzymatic activities of *ee*AChE, *h*AChE, and *h*GSK3 β by the isonicotinamide series of compounds (**11a–11j**).



Compd.	R1	X	n	R2	IC ₅₀ (μM)		
					<i>ee</i> AChE	<i>h</i> AChE	<i>h</i> GSK-3 β
11a	Cyclopropyl	N	1	–	0.0016	0.0026	0.023
11b	cyclopropyl	N	1	2-F	0.0101	0.0047	0.077
11c	cyclopropyl	N	1	4-F	0.0118	0.0010	0.031
11d	cyclopropyl	N	1	2-Cl	0.0972	0.0816	0.079
11e	cyclopropyl	N	0	–	9.806	>10	0.734
11f	Methyl	N	1	4-F	0.016	0.009	3.508
11g	cyclopropyl	CH	1	–	0.843	1.394	9.748
11h	cyclopropyl	CH	1	4-F	>10	n. d.	>10
11i	Methyl	CH	1	–	2.197	>10	>10
11j	Methyl	CH	1	4-F	>10	n. d.	>10

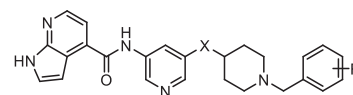
inhibitory ability of these four compounds against AChE did not improve as significantly as expected (Table 4). Rather, the inhibitory activity of this series of compounds on GSK3 β decreased significantly. Their preferred order was the formamide bond (**12a**) > amide bond (**12b**) > ether bond (**12d**), indicating that cyclopropanoyl was critical and unlikely amenable for further optimization.

Based on the results of four rounds of structural modifications and SAR discussion, **11a** and **11c** were selected as representative AChE/GSK3 β inhibitors with high activities for further exploration of *in vitro* and *in vivo* safety and efficacy.

Cholinesterase and kinase selectivity profiling of 11c. In addition to AChE, butyrylcholinesterase (BChE) is another hydrolyase of ACh that acts as the main hydrolyase of acetylcholine in the middle and later stages of AD [35]. The evaluation of the BChE inhibitory activity of compound **11c** revealed a lesser inhibition against BChE as compared to that against AChE; the IC₅₀ value was 5.3 μM. Thus, it exhibited a high selectivity index (SI = 5300) (Table S1). The structure of compound **11c** contained a 2-

Table 4

Inhibition of the enzymatic activities of *ee*AChE, *h*AChE and *h*GSK-3 β by the pyridopyrazole series of compounds (**12a–12d**).



Compd.	X	R	IC ₅₀ (μM)		
			<i>ee</i> AChE	<i>h</i> AChE	<i>h</i> GSK-3 β
12a		3-Cl	0.874	1.306	>10
12b		–	0.311	0.358	6.804
12c		4-F	0.406	0.227	4.935
12d		–	0.0023	0.0039	0.837

aminopyridine fragment, which is a common fragment in ATP competitive inhibitors [36]. Hence, the kinase selectivity profile of **11c** was examined on the CMGC kinase family of the CP kinase panel that shares high homology with GSK3 β (ChemPartner). This testing determined that 0.3 μM of compound **11c** displayed no significant inhibitory activity toward 18 related kinases, including the CDK family and P38 family (Fig. 5). The acceptable kinase selectivity of **11c** towards GSK3 may be attributed to the high selectivity (Fig. S4 in Supporting Information) of the parent compound **8** and the introduction of the benzylpiperidine group.

In vivo BBB penetration and pharmacokinetic evaluation. Considering that the target of the compounds was located in the central nervous system (CNS), the brain penetration study was performed by parallel artificial membrane permeation assay (PAMPA) and brain permeability in mice. The *in vitro* PAMPA results

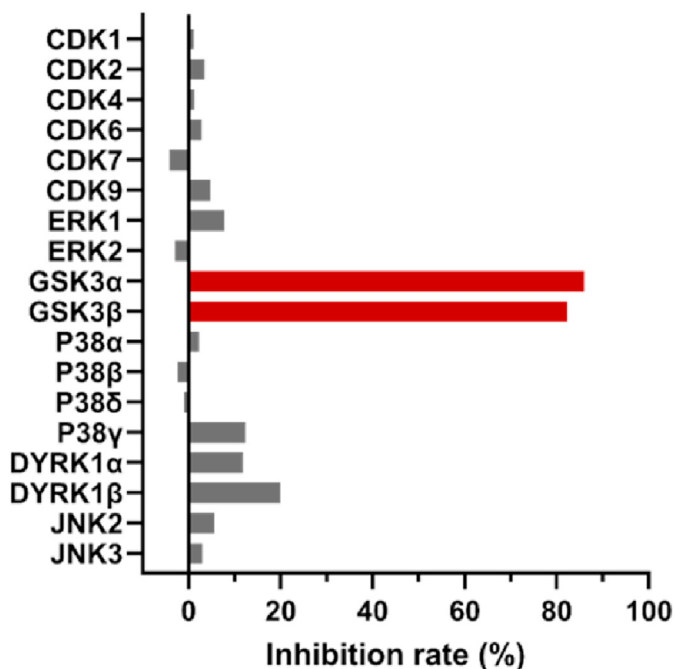


Fig. 5. The kinase selectivity profile of **11c** on the CMGC kinase family of CP kinase panel. **11c** was screened at a 300 nM concentration on an 18-kinase panel.

indicated that compounds **11a** and **11c** exhibited good BBB permeability with Pe (effective permeability coefficient) values of $8.2 \times 10^{-6} \text{ cm s}^{-1}$ and $10.5 \times 10^{-6} \text{ cm s}^{-1}$, respectively (Fig. S5 in Supporting Information). Further, the brain permeability of compounds was evaluated in ICR mice. After an oral administration of a 10 mg/kg dose, the concentrations of the two compounds in the brain and plasma were measured after 1 and 1.5 h of administration. As shown in Table 5, the concentration of compound **11a** in the brain was 34.4 ng/g after 1 h of administration and further increased to 43.7 ng/g after 1.5 h of administration with a brain/plasma ratio of 0.69. Compound **11c** exhibited a good concentration (62.0 ng/g) in the brain after 0.5 h. By extending the administration time, the concentration of **11c** in the brain tissue reached 113.1 ng/g, and a brain/plasma ratio of 0.39 was observed after 1.5 h of administration.

Compounds **11a** and **11c** were injected in a single dose of 10 mg/kg by oral (p.o.) or 1 mg/kg by intravenous (i.v.) administration in male SD rats, and the results are summarized in Table 6. Compound **11a** displayed moderate plasma exposure ($AUC_{0-\text{inf}} = 376.8 \text{ ng h/mL}$), and maximum serum concentration ($C_{\text{max}} = 47.1 \text{ ng/mL}$) following oral administration. Remarkably, compound **11c** displayed better plasma exposure ($AUC_{0-\text{inf}} = 1261.8 \text{ ng h/mL}$) and acceptable maximum serum concentration ($C_{\text{max}} = 158.6 \text{ ng/mL}$) after oral administration of 10 mg/kg. A moderate oral bioavailability (F) with a value of 31.0% was observed. Taken together, the favorable pharmacokinetic properties and high brain penetration capacity of compound **11c**, warrant its therapeutic potential in AD

Table 5
Brain Penetration Study for Compounds 11a and 11c (10 mg/kg p.o.) in ICR Mice.

compd.	Time (h)	Brain (ng/g)	Plasma (ng/g)	B/P ratio (100%)
11a	1	34.4 ± 2.7	112.2 ± 4.7	30.6
	1.5	43.7 ± 4.1	62.9 ± 3.0	69.5
11c	1	62.0 ± 5.8	405.2 ± 26.5	15.3
	1.5	113.1 ± 9.2	342.7 ± 19.1	33.0

and relative diseases.

Neuroprotection. Neuroprotection is a crucial property for anti-AD drugs. It entails the preservation of the neuronal structure and functionality and reduces neuronal loss and degeneration. Glutamate, an excitatory neurotransmitter, can lead to excitotoxicity and neuronal death [37]. During the course of AD, glutamatergic synapses are over-activated and induce excitotoxicity resulting in neuronal loss and synaptic plasticity damage. Therefore, the potential neuroprotective activity of the optimal compounds was explored against glutamate-induced damages in the mouse hippocampal neuron HT-22 cells. HT-22 cells were first incubated with compounds **11a** and **11c** (6 μM) for 1 h, and then cultured for the next 24 h with glutamate (18 mM). As shown in Fig. 6A and B, the morphology of the glutamate-treated cells shrank, resulting in approximately 58% of cell mortality compared to the control group. Compound **11c** alleviated the glutamate-induced cell damage and death (cell mortality reduced from 58% to 66%).

Synaptophysin, a fibrous phosphoprotein, is mainly located in the presynaptic vesicles of neuronal axons and may participate in the formation and exocytosis of the synaptic vesicles. Correlation between synaptophysin loss and the level of synaptic degeneration was previously reported for various experimental AD models [38]. It has been reported that activated GSK3 β can cause axonal contraction and synaptic damage; thus, leading to neuronal damage. Therefore, the above compounds were tested for their efficacy in preventing synaptic degeneration in HT-22 cells. An HT-22 cells model with low synaptophysin expression was established by induction with glutamate (6 mM) for 24 h; no significant cell death was caused. As expected, the HT-22 cells incubated with compound **11c** (6 μM) showed significantly elevated levels of synaptophysin compared with the glutamate-induced group (Fig. 6C). The effect of the compound on hippocampal synaptophysin was further evaluated in an A β 42-stimulated SD rat model [39]. The oligomerized A β 42 peptide (10 μg) was injected into the hippocampus (final coordinates from bregma anterior-posterior (AP): -6.0 mm; medial-lateral (ML): -5.0 mm; dorsal-ventral (DV): -3.2 mm) [40], and the rats were administered (5 mg/kg/day) for five consecutive days. The expression of synaptophysin on the hippocampal region was determined using immunohistochemical staining. Synaptophysin was stained red, and the nucleus was blue (Fig. 6D). Brains injected with A β 42 (10 μg) caused a decreased level of synaptophysin in the hippocampus compared with controls. After five days of administration of compound **11c** (5 mg/kg/day, p. o.), the synaptic density on the hippocampus increased compared with that of the brains injected with A β 42 alone (Fig. 6D, the red staining). These results indicated that compound **11c** enhanced synaptic survival in an A β 42-stimulated inflammatory environment.

Microtubule-associated protein tau promotes the assembly and stabilization of microtubules. GSK3 β is one of the key kinases for phosphorylation of the tau protein. Hyperphosphorylated tau causes unstable microtubules leading to NFTs. Therefore, the effects of **11c**-mediated inhibition of GSK3 β on the phosphorylation of tau protein were also tested in neuroblastoma N2a cells overexpressing human tau. As shown in Fig. 7, incubation with compound **11c** did not significantly change the level of phosphorylated (Ser396 epitope) tau (concentration less than 0.9 μM) for 6 h. Increasing the concentration of the compound to 0.9, 3, or 9 μM resulted in a dose-dependent decrease of phosphorylated tau protein.

In vivo measurement of AChE activity and levels of ACh. The pharmacodynamic evaluation of the activity of AChE and the level of ACh in the brain may be critical for the development of AChE inhibitors. Initially, the whole brains of ICR mice were immersed in different concentrations (5 μM , 10 μM , and 40 μM) of the compounds for 1 h, and the AChE activity in the brain tissue was tested using the Ellman method (the BChE activity was inhibited using

Table 6
Pharmacokinetic parameters for compounds 11a and 11c in rat.^a

Compd.	11a		11c	
Dose (mg/kg)	10	1	10	1
Dose route	p.o.	i.v.	p.o.	i.v.
AUC _{0-inf} (ng h/mL)	376.8 ± 41.0	152.0 ± 13.7	1261.8 ± 104.6	406.7 ± 25.8
C _{max} (ng/mL)	47.1 ± 4.9	98.3 ± 12.4	158.6 ± 19.2	199.7 ± 22.4
T _{max} (h)	1.7 ± 0.1	—	1.9 ± 0.2	—
t _{1/2} (h)	6.3 ± 0.4	21.4 ± 1.8	7.6 ± 0.6	5.2 ± 0.4
MRT _{0-inf} (h)	8.9 ± 2.1	10.0 ± 1.4	10.9 ± 9.2	5.1 ± 0.3
F (%)	24.8	—	31.0	—

^a AUC, area under the concentration-time curve; MRT, mean residence time. All values are represented as the mean ± SEM.

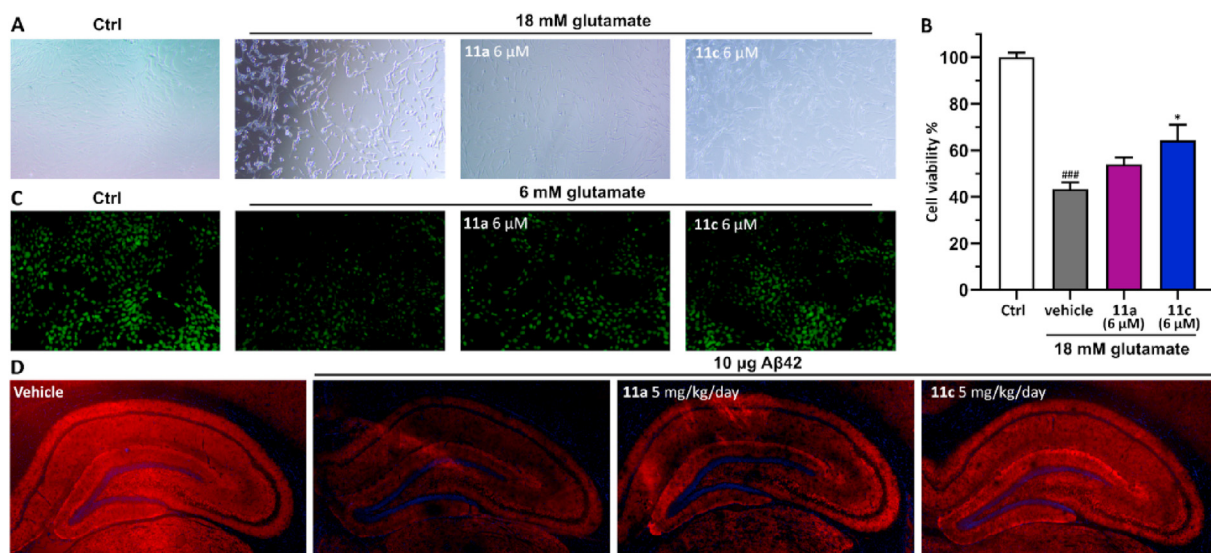


Fig. 6. The neuroprotective effects of **11c** in HT-22 cells. (A) The effect **11c** on glutamate-induced cell death in HT-22 cells. (C) Immunocytochemistry for synaptophysin (synaptic connections) on glutamate-induced cell death in HT-22 cells. (D) Immunohistochemistry for synaptophysin (red staining) on hippocampus in an A β 42-stimulated SD rat model.

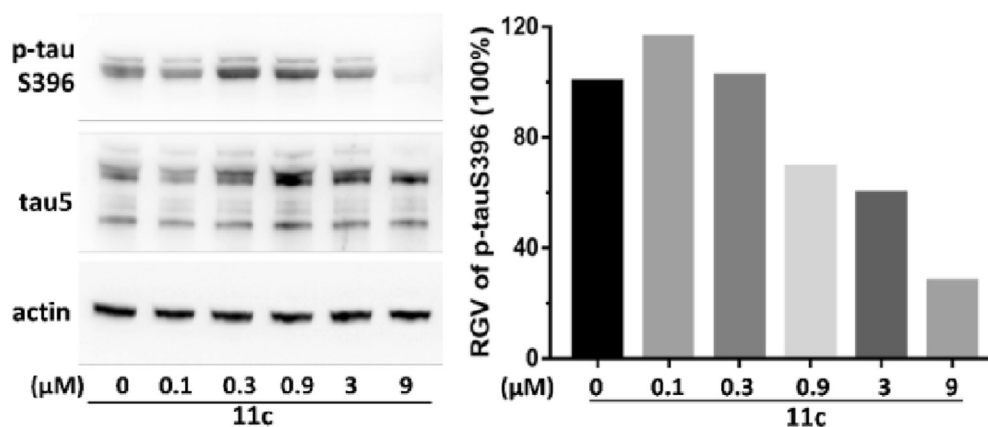


Fig. 7. The effect of **11c** on tau phosphorylation at Ser396 in N2a cells overexpressing human tau. The ratio (RGV) of phosphorylated tau to tau 5 protein was quantified using ImageJ analysis software.

100 μ M ethopropazine hydrochloride). As shown in Fig. 8B, the compounds inhibited the activity of AChE in the brain in a dose-dependent manner. Compound **11c** significantly inhibited the AChE activity at 40 μ M and displayed a slight increase in the potency relative to compound **11a** (75.3% vs. 63.7%). Moreover, to further evaluate whether these compounds could cross the BBB and inhibit the activity of AChE in the brain, the whole brain, and intestine of ICR mice were collected after 1.5 h of the administration

of compound **11a**, **11c**, or donepezil (10 mg/kg, p. o.). Compound **11c** significantly inhibited acetylcholinesterase in the brain compared to **11a** (53.8% vs 26.9%), and this may be attributed to the considerable brain exposure of compound **11c** (Fig. 8C). Donepezil has a strong inhibitory effect on AChE activity in the brain. However, it showed a strong inhibitory effect on AChE in the intestinal tissue as well. The gastrointestinal side effects caused by donepezil were reported to be associated with the inhibition of the peripheral

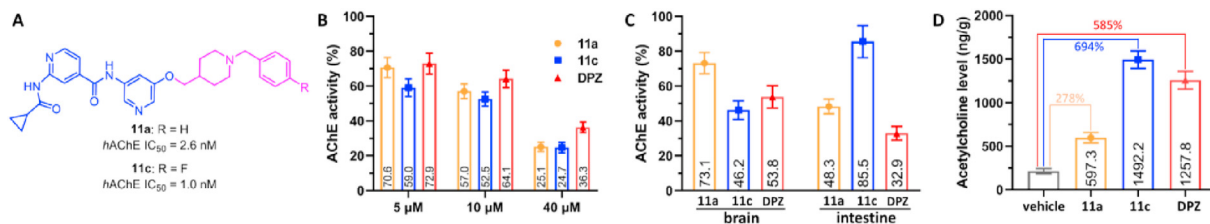


Fig. 8. The effects of compounds **11a**, **11c** and donepezil (DPZ) on AChE activity and ACh level in mouse brain. (B) After the brain was immersed in the compound for 1 h, the activity of AChE in the brain. (C) After mice was administered compound (p.o., 10 mg/kg) for 1.5 h, the activity of AChE in the brain and intestine. (D) The level of ACh in the brain after mice was administered compound (p.o., 10 mg/kg) for 1.5 h.

cholinergic receptors. It is worth noting that the inhibitory rate of compound **11c** on intestinal AChE was significantly lower than that of donepezil (14.5% vs. 67.1%). This reduced inhibitory rate of **11c** is expected to alleviate the intestinal side effects caused by donepezil.

Considering the important role of the ACh neurotransmitter in learning and memory, the effect of the compounds was evaluated on the ACh levels in the brain of ICR mice by HPLC-MS/MS (Fig. S6 in Supporting Information). The measurement results of ACh levels (Fig. 8D) depict the mean baseline extracellular ACh levels of 215.0 ng/g in the whole brain. After oral administration of compound **11c** (10 mg/kg) for 1.5 h, the extracellular ACh levels increased approximately 694%; this value was slightly higher than that of donepezil (1492.2 ng/g vs 1257.8 ng/g).

Ameliorative effect of compound 11c on cognitive impairments. Since scopolamine, an antagonist of the muscarinic acetylcholine receptor, can induce cholinergic deficits and cognitive impairment, the scopolamine-induced amnesic mouse model is widely used to evaluate the effectiveness of cholinergic agents, especially AChE inhibitors [41]. In the present study, a channel water maze was employed to assess the cognitive behavior of mice. In the probe trial, mice injected intraperitoneally with scopolamine (4 mg/kg) showed significantly increased escape latency (Fig. 9A) and a more chaotic trajectory to the target (Fig. S7 in Supporting Information). In contrast, compounds **11a**, **11c**, and donepezil

(10 mg/kg/day, p. o.) significantly shortened the latency and simplified the tracks to the target in the scopolamine-stimulated mice ($P < 0.01$, $P < 0.001$, and $P < 0.001$, respectively). Particularly, the target latency of the compound **11c** group was similar to that of the blank group (18.1 s vs 17.9 s).

Further, the performances in the Y-maze and Morris water maze were assessed to determine the ameliorative effects of compound **11c** on the Aβ42 intracerebroventricular (icv) injection model [42]. The spontaneous alternation performance of Aβ42-treated mice was significantly reduced in the Y-maze test (Fig. 9B). Compound **11c** and donepezil rescued the Aβ42-induced spontaneous working memory impairment ($P < 0.001$). To assess memory retention, the platform was removed, and the spatial probe trial test was conducted after five days of the training trial (Fig. S7). The saline group displayed a good memory for the position of the platform: about seven times of crossing the platform in the 120-s free space exploration test (Fig. 9C and D). In contrast, the Aβ42-induced mice exhibited a poor memory for the position of the platform and made aimless movements around the edge of the pool. Compound **11c** and donepezil significantly ameliorated the spatial learning and memory impairment in the Aβ42-induced mice: the number of crossing platforms was increased to 7 times in the probe trial ($P < 0.01$).

Safety. During the entire behavioral evaluation period,

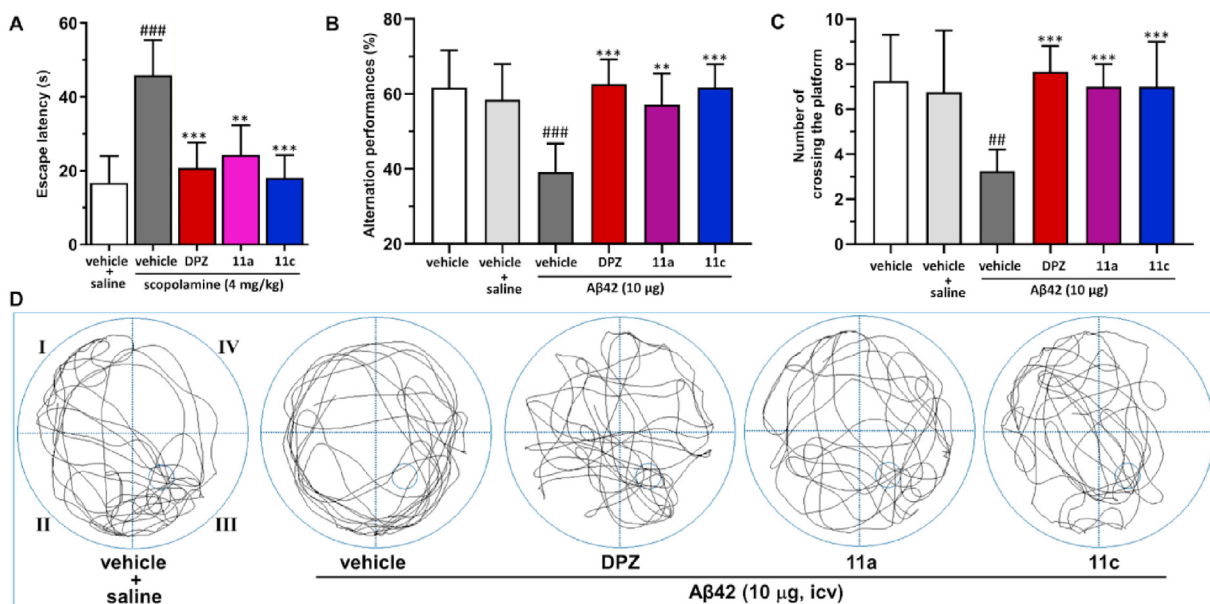


Fig. 9. Effects of compound **11c** (p.o.) on scopolamine-induced (A) or Aβ42 peptide-induced (B–D) cognitive deficits. (A) Escape latencies (time to find the escape platform) in Morris water maze; (B) Spontaneous alternation performances in Y maze. (C) The number of platforms crossed in the probe trial. (D) After the platform was removed, the motion trajectory diagram of mouse in 120 s. Data were presented as mean ± SEM (N = 8–10). ### $P < 0.001$ vs the control group (vehicle + saline); ** $P < 0.01$, *** $P < 0.001$ vs the model group.

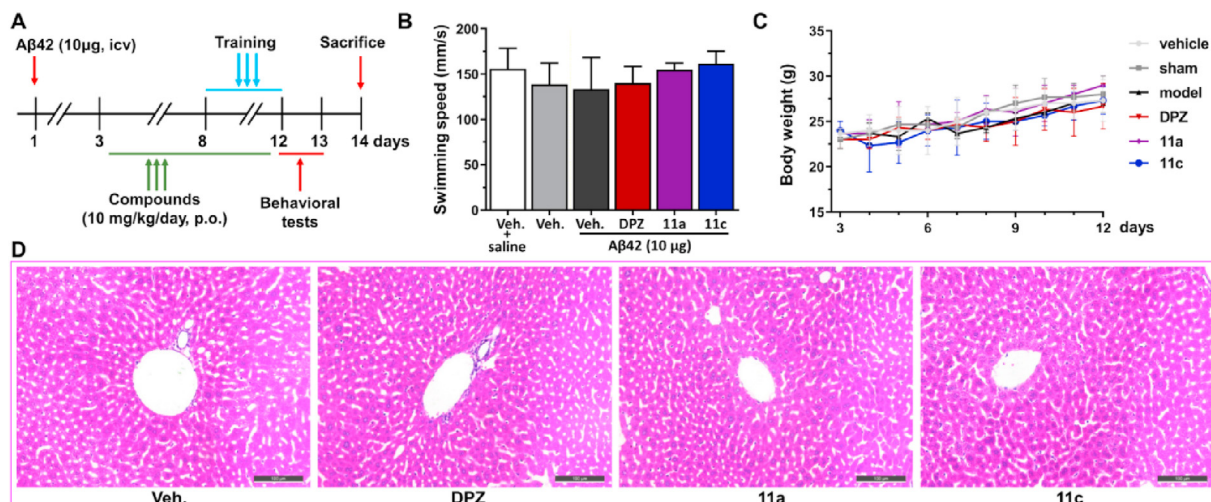


Fig. 10. Safety evaluation of the compound in ICR mice. (A) Experimental protocols. (B) The swimming speeds of mice. (C) The mean daily body weight profile of mice during the drug administration period ($n = 8-10$). (D) Histomorphological appearance of livers of mice after administration of compound. HE staining, original magnification $\times 200$.

compound **11c** (10 mg/kg/day, p. o.) did not cause any obvious abnormalities in the body weight or swimming speed. This indicated that a continuous administration of the compound may have little effect on the metabolism and normal behavior of the mice (Fig. 10B and C). After the behavioral experiment, the hepatotoxicity of the compounds was further evaluated by immunohistochemical staining. The morphologic studies demonstrated that compound **11c** did not present obvious morphologic changes in the liver compared to the control group (Fig. 10D).

3. Conclusions

The drugs used in the treatment of mild-to-moderate AD are mainly AChE inhibitors based on the cholinergic hypothesis, and their efficacy has been clinically confirmed. However, with the atrophy of the hippocampus and the enlargement of ventricles in AD patients, the cholinergic neurons and synapses disappear. This reduces the effect of increasing ACh level by inhibiting AChE. Therefore, the combination of AChE inhibitors and neuroprotective agents may produce a better anti-AD effect. The combination therapy of donepezil and the neuroprotective agent memantine (Namzaric®) was approved in 2014 for the treatment of moderate to severe AD patients.

A large number of studies have confirmed that GSK3 β plays an important role in the induction of neuronal injuries such as neuroinflammation, NFTs, and synaptic damage. Previously, a total of 60 AChE/GSK3 β inhibitors were synthesized by our group based on acylaminopyridine pharmacophores, and valuable information on the SAR was accumulated. Here, a new skeleton of AChE/GSK3 β inhibitors has been disclosed. Among them, compound **11c** with an isonicotinamide core design was identified as a potent dual AChE/GSK3 β inhibitor with high blood-brain barrier permeability. Oral administration of compound **11c** also exhibited a strong inhibitory effect on the AChE in the brain of mice. It should be noted that compound **11c** displayed weaker inhibitory activity against AChE in the peripheral tissues such as the intestine compared with its action in the central nervous system. Additionally, oral administration of **11c** significantly elevated the level of ACh in the brain of mice and ameliorated the cognitive and learning abilities in scopolamine- or A β 42-induced cognitive deficit models. Finally, compound **11c** also exerted potent neuroprotective effects, including glutamate-stimulated HT-22 neurotoxicity, tau protein phosphorylation, and

A β 42-induced synaptophysin loss in rat hippocampus. These favorable outcomes demonstrate that compound **11c** deserves further optimization as advanced probe.

4. Experimental section

4.1. Chemistry

All solvents and chemicals were purchased from commercial sources and used directly without further purification. Anhydrous THF (99.5%, extra dry, with molecular sieves, stabilized with BHT, water ≤ 50 ppm) was purchased from Energy Chemical. All reactions were performed under an argon atmosphere. Thin-layer chromatography (TLC) plates was performed on silica gel 60 GF²⁵⁴ and visualized with ultraviolet light (254 and 365 nm). Flash chromatography was performed on 300–400 mesh silica gel (Fisher Scientific). NMR spectra were recorded on a Bruker Avance III 300, or 500 MHz spectrometer (Bruker Biospin AG) with tetramethylsilane (TMS) as an internal standard, and chemical shifts were reported in parts per million (ppm, δ). HRMS were measured on Agilent G6520 Q-TOF. The purity of the compounds was determined by HPLC (LCMS 2020 from Shimadzu). The purity of all target products is more than 95%.

General procedure for the synthesis of target compounds

9a–9b. Carboxylic acid derivative **13** (5 g, 20.747 mmol) was dissolved in *N,N*-dimethylformamide (DMF). Dicyclohexylcarbodiimide (DCC) (4.7 g, 22.816 mmol), 1-hydroxybenzotriazole (HOBT) (3.22 g, 23.852 mmol) and amino derivative **14** (5.32 g, 24.860 mmol) was added. The reaction was stirred at room temperature for 24 h. The solvent was removed, and the residue was resolved in ethyl acetate (EA). The organic phase was washed with water ($3 \times$), 2 N aqueous HCl ($1 \times$), and brine ($1 \times$). After drying over MgSO₄ and filtration, the organic solvent was evaporated under reduced pressure. The solid was purified by flash chromatography to give intermediate **15**. White powder (84%). ¹H NMR (300 MHz, DMSO-*d*₆) δ 13.82 (s, 1H), 8.58 (t, $J = 6.0$ Hz, 1H), 8.34 (s, 1H), 7.65 (d, $J = 8.3$, 1H), 7.56 (d, $J = 8.3$, 1H), 3.94 (d, $J = 15.0$, 2H), 3.21 (t, $J = 6.0$, 2H), 2.70 (br s, 2H), 1.79 (br s, 1H), 1.67 (d, $J = 12.0$, 2H), 1.41 (s, 9H), 1.11–0.99 (m, 2H). MS (ESI) m/z : 436.1 [M – H][–].

Intermediate **15** (437 mg, 1 mmol), 3-pyridineboronic acid (488 mg, 4 mmol), Pd (dppf)Cl₂ (183 mg, 0.25 mmol), Cs₂CO₃ (1.3 g, 4 mmol) were added to the schlenk reaction tube. Subsequently,

40 mL of mixed solvent (1,4-dioxane/water = 3:1 (v/v)) was added in an argon atmosphere. The reaction was stirred at 115 °C for 24 h. The solvent was removed, and the residue was resolved in MeOH and filtered to remove palladium. The filtrate was purified by flash chromatography to give intermediate **16**. Light yellow solid (73%). ¹H NMR (300 MHz, DMSO-*d*₆) δ 13.74 (br s, 1H), 8.92 (d, *J* = 2.0 Hz, 1H), 8.61–8.55 (m, 2H), 8.45 (s, 1H), 8.13 (d, *J* = 8.3, 1H), 7.82–7.75 (m, 2H), 7.56–7.52 (m, 1H), 3.95 (d, *J* = 15.0, 2H), 3.24 (t, *J* = 6.0, 2H), 2.71 (br s, 2H), 1.81 (br s, 1H), 1.69 (d, *J* = 12.0, 2H), 1.41 (s, 9H), 1.13–1.01 (m, 2H). MS (ESI) *m/z*: 434.1 [M – H[−]].

N-((1-benzylpiperidin-4-yl)methyl)-5-(pyridin-3-yl)-1*H*-indazole-3-carboxamide (**9a**). To a solution of **15** (153 mg, 352 μmol) in 5 mL dry DCM, 2 mL of trifluoroacetic acid (TFA) was added at 0 °C. The reaction solution was stirred at room temperature for 3 h. Subsequently, the reaction solution was concentrated and dissolved in DMF (12 mL). K₂CO₃ (97 mg, 0.703 mmol) and benzyl bromide (51 μL, 0.425 mmol) were added. The reaction solution was stirred at 55 °C for 5 h. The solvent was removed, and the residue was purified by flash chromatography to give **9a**. Light yellow solid (59%). ¹H NMR (300 MHz, Chloroform-*d*) δ 8.91 (d, *J* = 2.3 Hz, 1H), 8.65 (d, *J* = 1.7 Hz, 1H), 8.60 (dd, *J* = 4.8, 1.6 Hz, 1H), 7.97 (dt, *J* = 8.0, 2.0 Hz, 1H), 7.62 (dd, *J* = 8.8, 1.7 Hz, 1H), 7.45 (d, *J* = 8.8 Hz, 1H), 7.36–7.33 (m, 5H), 7.23 (m, 2H), 7.21 (s, 1H), 3.57 (s, 2H), 3.43 (t, *J* = 6.3 Hz, 2H), 2.97 (m, 2H), 2.06 (td, *J* = 11.6, 2.4 Hz, 2H), 1.90–1.77 (m, 2H), 1.76–1.71 (m, 1H), 1.50 (td, *J* = 12.4, 4.0 Hz, 2H). ¹³C NMR (75 MHz, DMSO-*d*₆) δ 162.2, 148.7, 148.3, 140.8, 138.6, 137.3, 136.3, 134.9, 132.3, 131.2, 129.2, 128.6, 128.2, 127.7, 127.0, 124.4, 123.5, 120.6, 111.9, 53.3, 52.9, 49.1, 30.2. HRMS (ESI): (M + H)⁺ calcd for C₂₆H₂₈N₅O, 426.2288; found, 426.2288.

N-((1-(2-fluorobenzyl)piperidin-4-yl)methyl)-5-(pyridin-3-yl)-1*H*-indazole-3-carboxamide (**9b**). Compound **9b** (52%) was synthesized by a procedure similar to that used to prepare compound **9a** as a light yellow solid. ¹H NMR (300 MHz, DMSO-*d*₆) δ 8.90 (s, 1H), 8.57 (d, *J* = 4.8 Hz, 1H), 8.53 (t, *J* = 6.1 Hz, 1H), 8.43 (s, 1H), 8.09 (d, *J* = 7.9 Hz, 1H), 7.76 (s, 2H), 7.50 (dd, *J* = 8.0, 4.8 Hz, 1H), 7.37 (t, *J* = 7.1 Hz, 2H), 7.15 (t, *J* = 8.7 Hz, 2H), 3.60 (s, 2H), 3.21 (d, *J* = 6.3 Hz, 2H), 2.95–2.78 (m, 2H), 2.11 (s, 2H), 1.72 (m, 1H), 1.68 (m, 2H), 1.30–1.20 (m, 2H). ¹³C NMR (75 MHz, DMSO-*d*₆) δ 162.13, 160.31 (d, ¹*J*_{C-F} = 245.7 Hz), 148.75, 148.30, 140.99, 138.89, 134.90, 132.34, 130.60 (d, ³*J*_{C-F} = 8.2 Hz), 130.12, 127.07, 125.30, 124.63, 124.11 (d, ³*J*_{C-F} = 14.7 Hz), 123.41, 120.58, 116.05 (d, ²*J*_{C-F} = 20.6 Hz), 115.57 (d, ²*J*_{C-F} = 22.3 Hz), 111.73, 55.14, 53.20, 47.01, 44.39, 30.16. HRMS (ESI): (M + H)⁺ calcd for C₂₆H₂₇FN₅O, 444.2194; found, 444.2198.

General procedure for the synthesis of target compounds 9c–9e. Carboxylic acid derivative **18** (2.005 g, 8.251 mmol) was dissolved in 200 mL of DMF, *N,N*-diisopropylethylamine (DIPEA) (4.31 mL, 24.724 mmol), 1*H*-benzene benzotriazole-1-yl-oxy-tripyrrolidinophosphonium hexafluorophosphate (PyBOP) (6.435 g, 12.375 mmol), HOBT (1.782 g, 13.200 mmol) and amine derivative **17** (3.5 g, 16.509 mmol) was added. The reaction solution was stirred at room temperature for 12 h in an argon atmosphere. The solvent was removed, and the residue was resolved in ethyl acetate (EA). The organic phase was washed with water (3 ×), 2 N aqueous HCl (1 ×), and brine (1 ×). After drying over MgSO₄ and filtration, the organic solvent was evaporated under reduced pressure. The solid was purified by flash chromatography to give intermediate **19**. White powder (83%). ¹H NMR (300 MHz, DMSO-*d*₆) δ 8.72 (br s, 1H), 8.59 (br s, 1H), 8.30 (d, *J* = 2.1 Hz, 1H), 7.72 (dd, *J* = 8.0, 2.1 Hz, 1H), 7.64 (d, *J* = 8.0 Hz, 1H), 3.92 (d, *J* = 13.1 Hz, 2H), 2.89 (d, *J* = 6.9 Hz, 2H), 2.09–2.01 (m, 1H), 1.75–1.64 (m, 2H), 1.40 (s, 9H), 1.11 (qd, *J* = 12.3, 11.4, 3.4 Hz, 2H). MS (ESI) *m/z*: 436.1 [M – H[−]].

Tert-butyl 4-(2-oxo-2-((6-(pyridin-3-yl)-1*H*-indazol-3-yl)amino)ethyl)piperidine-1-carboxylate (**20**). Intermediate **20** (81%) was synthesized by a procedure similar to that used to prepare

intermediate **16** as a light yellow solid. ¹H NMR (300 MHz, DMSO-*d*₆) δ 8.92 (d, *J* = 2.3 Hz, 1H), 8.63 (dd, *J* = 6.2, 2.3 Hz, 1H), 8.51 (m, 1H), 8.11 (dt, *J* = 6.2, 2.3 Hz, 1H), 8.01 (d, *J* = 8.1 Hz, 1H), 7.69 (dd, *J* = 8.2, 1.6 Hz, 1H), 7.53 (dd, *J* = 8.0, 4.6 Hz, 1H), 6.58 (s, 2H), 3.93 (d, *J* = 12.7 Hz, 2H), 2.92 (d, *J* = 6.9 Hz, 2H), 2.74 (br s, 2H), 2.12–2.04 (m, 1H), 1.72 (dd, *J* = 13.5, 3.4 Hz, 2H), 1.39 (s, 9H), 1.17–1.05 (m, 1H). MS (ESI) *m/z*: 434.1 [M – H[−]].

2-(1-Benzylpiperidin-4-yl)-*N*-(6-(pyridin-3-yl)-1*H*-indazol-3-yl)acetamide (**9c**). Compound **9c** (52%) was synthesized by a procedure similar to that used to prepare compound **9a** as a light yellow solid. ¹H NMR (300 MHz, DMSO-*d*₆) δ 8.92 (d, *J* = 9.0 Hz, 1H), 8.62 (d, *J* = 6.1 Hz, 1H), 8.51 (s, 1H), 8.12 (d, *J* = 6.1 Hz, 1H), 8.02 (d, *J* = 7.9 Hz, 1H), 7.68 (d, *J* = 9.0 Hz, 1H), 7.53 (dd, *J* = 9.0, 6.0 Hz, 1H), 7.34–7.31 (m, 4H), 7.26–7.21 (m, 1H), 6.58 (s, 2H), 3.46 (s, 2H), 2.91 (d, *J* = 6.3 Hz, 2H), 2.80 (d, *J* = 9.0 Hz, 2H), 2.03–1.95 (m, 1H), 1.94–1.89 (m, 2H), 1.72 (dd, *J* = 12.0, 3.1 Hz, 2H), 1.37–1.23 (m, 2H). ¹³C NMR (75 MHz, DMSO-*d*₆) δ 170.8, 152.5, 149.0, 148.0, 139.9, 138.8, 138.2, 135.6, 134.8, 128.9, 128.2, 127.0, 124.1, 122.9, 121.6, 119.8, 113.3, 62.3, 53.0, 40.9, 32.1, 31.6. HRMS (ESI): (M + H)⁺ calcd for C₂₆H₂₈N₅O, 426.2288; found, 426.2293.

2-(1-(2-Fluorobenzyl)piperidin-4-yl)-*N*-(6-(pyridin-3-yl)-1*H*-indazol-3-yl)acetamide (**9d**). Compound **9d** (49%) was synthesized by a procedure similar to that used to prepare compound **9a** as a light yellow solid. ¹H NMR (300 MHz, DMSO-*d*₆) δ 8.91 (s, 1H), 8.61 (d, *J* = 4.7 Hz, 1H), 8.50 (s, 1H), 8.10 (d, *J* = 8.1 Hz, 1H), 8.01 (d, *J* = 3.0 Hz, 1H), 7.68 (d, *J* = 8.2 Hz, 1H), 7.54–7.50 (m, 1H), 7.38 (t, *J* = 7.4 Hz, 1H), 7.29 (t, *J* = 6.0 Hz, 1H), 7.22–7.09 (m, 2H), 6.58 (s, 2H), 3.47 (s, 2H), 2.90 (d, *J* = 6.8 Hz, 2H), 2.78 (d, *J* = 11.0 Hz, 3H), 2.51 (s, 1H), 1.97 (t, *J* = 11.7 Hz, 2H), 1.92–1.85 (m, 1H), 1.70 (d, *J* = 12.6 Hz, 2H), 1.34–1.25 (m, 2H). ¹³C NMR (75 MHz, DMSO-*d*₆) δ 171.07, 161.20 (d, ¹*J*_{C-F} = 244.4 Hz), 152.89, 149.38, 148.45, 140.28, 139.16, 136.06, 135.20, 131.88 (d, ³*J*_{C-F} = 4.7 Hz), 129.34 (d, ³*J*_{C-F} = 8.3 Hz), 125.37 (d, ²*J*_{C-F} = 14.4 Hz), 124.57, 124.53, 124.45, 123.32, 121.97, 120.16, 115.53 (d, ²*J*_{C-F} = 21.9 Hz), 113.67, 55.31, 53.40, 41.36, 32.52, 32.22. HRMS (ESI): (M + H)⁺ calcd for C₂₆H₂₇FN₅O, 444.2194; found, 444.2196.

2-(1-(4-Fluorobenzyl)piperidin-4-yl)-*N*-(6-(pyridin-3-yl)-1*H*-indazol-3-yl)acetamide (**9e**). Compound **9e** (58%) was synthesized by a procedure similar to that used to prepare compound **9a** as a light yellow solid. ¹H NMR (300 MHz, DMSO-*d*₆) δ 8.90 (d, *J* = 2.3 Hz, 1H), 8.61 (dd, *J* = 4.8, 1.5 Hz, 1H), 8.50 (d, *J* = 1.4 Hz, 1H), 8.10 (dt, *J* = 8.0, 2.0 Hz, 1H), 8.02 (d, *J* = 8.2 Hz, 1H), 7.67 (dd, *J* = 8.2, 1.5 Hz, 1H), 7.51 (dd, *J* = 7.9, 4.8 Hz, 1H), 7.35 (dd, *J* = 8.4, 5.7 Hz, 2H), 7.14 (t, *J* = 8.8 Hz, 2H), 6.59 (s, 2H), 3.57 (s, 0H), 2.91 (d, *J* = 6.9 Hz, 2H), 2.84 (d, *J* = 11.7 Hz, 3H), 2.10 (s, 2H), 2.00–1.88 (m, 1H), 1.79–1.66 (m, 2H), 1.33 (q, *J* = 10.9 Hz, 2H). ¹³C NMR (75 MHz, DMSO-*d*₆) δ 170.97, 161.90 (d, ¹*J*_{C-F} = 243.6 Hz), 158.71, 152.94, 149.38, 148.43, 140.28, 139.16, 136.05, 135.20, 131.54 (d, ³*J*_{C-F} = 6.6 Hz), 124.45, 123.34, 122.04, 120.20, 115.41 (d, ²*J*_{C-F} = 21.2 Hz), 113.64, 61.28, 53.03, 41.16, 32.16, 31.56. HRMS (ESI): (M + H)⁺ calcd for C₂₆H₂₇FN₅O, 444.2194; found, 444.2203.

4.2. General procedure for the synthesis of target compounds 10a–10 l

2-(Cyclopropanecarboxamido)isonicotinic acid (**22**). To a solution of compound **21** (6.08 g, 40 mmol) and K₂CO₃ (11.04 g, 80 mmol) in THF (200 mL) was slowly added cyclopropanecarbonyl chloride (7.2 mL, 80 mmol) wise over a period of 5 min in an ice bath. The mixture was allowed to stir at room temperature for 24 h. After complete reaction, K₂CO₃ was removed by filtration and methanol (60 mL) was added. After cooling, LiOH aqueous solution (24 mL, 3 mol/l) was added dropwise at 0 °C. The reaction solution was stirred at room temperature for 6 h. The organic solvent was removed and water (60 mL) was added. The pH of the solution was

adjusted to 5 using 3 N HCl. The intermediate **22** was filtered and dried as a white solid (81%). ^1H NMR (300 MHz, DMSO- d_6) δ 11.05 (s, 1H), 8.59 (s, 1H), 8.49 (d, $J = 5.1$ Hz, 1H), 7.52 (d, $J = 5.1$ Hz, 1H), 2.05 (t, $J = 6.1$ Hz, 1H), 0.87–0.84 (m, 4H).

Methyl 5-(2-(cyclopropanecarboxamido)isonicotinamido)nicotinate (23). The carboxylic acid derivative **22** (1.65 g, 8.0 mmol) was dissolved in DMF (30 mL). DIPEA (3.97 mL, 24.0 mmol), HATU (3.95 g, 10.4 mmol) and methyl 5-aminonicotinate (1.46 g, 9.6 mmol) were added under ice-water bath conditions. The reaction solution was stirred at room temperature for 24 h. EA was added to the reaction solution and the precipitate was filtered. The filtrate was concentrated and purified by flash chromatography to give intermediate **23** as a light yellow solid (52%). ^1H NMR (300 MHz, DMSO- d_6) δ 11.07 (s, 1H), 10.93 (s, 1H), 9.16 (d, $J = 2.5$ Hz, 1H), 8.86 (d, $J = 1.9$ Hz, 1H), 8.77 (t, $J = 2.2$ Hz, 1H), 8.57 (s, 1H), 8.54 (d, $J = 5.2$ Hz, 1H), 7.58 (dd, $J = 5.2, 1.5$ Hz, 1H), 3.92 (s, 3H), 2.09–2.01 (m, 1H), 0.87–0.82 (m, 4H).

5-(2-(Cyclopropanecarboxamido)isonicotinamido)nicotinic acid (24). Compound **23** (1.97 g, 5.8 mmol) was dissolved in THF/MeOH (3:1, v/v, 30 mL) solution, and NaOH aqueous solution (16 mL, 1 mol/l) was added dropwise under ice bath conditions. The reaction solution was stirred at room temperature for 7 h. The organic solvent was removed and water (30 mL) was added. The pH of the solution was adjusted to 5 with 3 N HCl. The intermediate **24** was filtered and dried as a white solid (80%). ^1H NMR (300 MHz, DMSO- d_6) δ 11.98 (br s, 1H), 11.02 (s, 1H), 8.41 (s, 1H), 8.37 (d, $J = 5.1$ Hz, 1H), 7.50–7.34 (m, 1H), 2.05–1.99 (m, 1H), 0.91–0.85 (m, 4H). MS (ESI) m/z : 325.1 [M – H] $^-$.

Tert-butyl 4-((5-(2-(cyclopropanecarboxamido)isonicotinamido)nicotinamido) methyl)piperidine-1-carboxylate (25a). To a solution of **24** (1.63 g, 5.0 mmol) in DMF (30 mL) was added DIPEA (2.48 mL, 15.0 mmol), followed by the addition of HATU (2.47 g, 6.5 mmol) and 4-(aminomethyl) piperidine-1-carboxylic acid tert butyl ester (1.29 g, 6.0 mmol) under ice bath conditions. After stirring for 24 h at room temperature, the resulting mixture the resulting mixture was dropped into 100 mL of ice water, and extracted by EA. The organic phase was concentrated and purified by flash chromatography to give intermediate **25a** as a light yellow solid (61%). ^1H NMR (300 MHz, DMSO- d_6) δ 11.09 (s, 1H), 10.88 (s, 1H), 9.09–9.00 (m, 1H), 8.84–8.75 (m, 2H), 8.58 (s, 2H), 8.54 (d, $J = 5.1$ Hz, 1H), 7.59 (dt, $J = 5.1, 1.4$ Hz, 1H), 3.95 (d, $J = 13.0$ Hz, 2H), 3.27–3.12 (m, 2H), 2.70 (s, 2H), 2.20–1.92 (m, 1H), 1.76 (s, 1H), 1.69 (d, $J = 14.4$ Hz, 2H), 1.07 (dd, $J = 13.9, 10.1$ Hz, 2H), 0.87 (d, $J = 4.7$ Hz, 4H). MS (ESI) m/z : 521.1 [M – H] $^-$.

5-(2-(Cyclopropanecarboxamido)isonicotinamido)-N-((1-(3-fluorobenzyl)piperidin-4-yl)methyl)nicotinamide (25b). Intermediate **25b** was synthesized using the same method as that for **25a** by reacting 4-amino-1-boc-piperidine with **24**. Light yellow solid (47%). ^1H NMR (300 MHz, DMSO- d_6) δ 11.07 (s, 1H), 10.87 (s, 1H), 9.06 (s, 1H), 8.78 (s, 1H), 8.57 (s, 3H), 8.54 (d, $J = 5.4$ Hz, 1H), 7.59 (d, $J = 5.3$ Hz, 1H), 3.96 (d, $J = 15.0$ Hz, 2H), 2.92–2.85 (m, 2H), 2.10–1.97 (m, 1H), 1.83 (d, $J = 12.9$ Hz, 2H), 1.53–1.49 (m, 2H), 1.43 (s, 9H), 0.87 (d, $J = 6.1$ Hz, 4H). MS (ESI) m/z : 507.2 [M – H] $^-$.

Tert-butyl 4-(2-(5-(2-(cyclopropanecarboxamido)isonicotinamido)nicotinamido) ethyl)piperidine-1-carboxylate (25c). Intermediate **25c** was synthesized using the same method as that for **25a** by reacting 4-amino-1-boc-piperidine with **24**. Light yellow solid (43%). ^1H NMR (300 MHz, DMSO- d_6) δ 11.07 (s, 1H), 10.42 (s, 1H), 9.10 (br s, 1H), 8.79 (br s, 1H), 8.58–8.56 (m, 2H), 8.55 (br s, 1H), 8.51 (s, 1H), 7.58 (d, $J = 5.8$ Hz, 1H), 3.44–3.42 (m, 2H), 3.30–3.28 (m, 2H), 2.83–2.81 (m, 2H), 2.03–2.01 (m, 1H), 1.99–1.97 (m, 1H), 1.91–1.89 (m, 2H), 1.62–1.60 (m, 2H), 1.25–1.21 (m, 2H), 1.43 (s, 9H), 0.89–0.84 (m, 4H). MS (ESI) m/z : 535.1 [M – H] $^-$.

N-((1-(benzyl)piperidin-4-yl)methyl)-5-(2-(cyclopropanecarboxamido)isonicotinamido) nicotinamide (10a).

Compound **10a** (63%) was synthesized by a procedure similar to that used to prepare compound **9a** as a light yellow solid. ^1H NMR (300 MHz, DMSO- d_6) δ 11.05 (s, 1H), 10.86 (s, 1H), 9.03 (d, $J = 2.4$ Hz, 1H), 8.76 (s, 1H), 8.73 (t, $J = 5.7$ Hz, 1H), 8.56 (s, 2H), 8.52 (d, $J = 5.1$ Hz, 1H), 7.57 (d, $J = 5.2$ Hz, 1H), 7.32 (d, $J = 4.3$ Hz, 4H), 7.26 (q, $J = 5.1, 4.4$ Hz, 1H), 3.18 (dd, $J = 8.3, 4.7$ Hz, 4H), 2.88 (d, $J = 11.1$ Hz, 2H), 2.09 (s, 1H), 2.03 (q, $J = 6.3$ Hz, 2H), 1.69 (d, $J = 13.2$ Hz, 2H), 1.60 (s, 1H), 1.29 (d, $J = 12.4$ Hz, 2H), 0.86 (s, 2H), 0.83 (d, $J = 2.6$ Hz, 2H). ^{13}C NMR (125 MHz, DMSO- d_6) δ 173.4, 165.3, 165.2, 153.3, 149.1, 144.4, 143.9, 143.8, 135.6, 130.7, 129.6, 128.7, 127.7, 127.0, 124.6, 117.4, 112.0, 55.4, 53.1, 49.1, 30.8, 29.4, 14.7, 8.3. HRMS (ESI): (M + H) $^+$ calcd for C₂₉H₃₃N₆O₃, 513.2609; found, 513.2609.

5-(2-(Cyclopropanecarboxamido)isonicotinamido)-N-((1-(2-fluorobenzyl)piperidin-4-yl)methyl)nicotinamide (10b). Compound **10b** (55%) was synthesized by a procedure similar to that used to prepare compound **9a** as a light yellow solid. ^1H NMR (300 MHz, DMSO- d_6) δ 11.07 (s, 1H), 10.86 (s, 1H), 9.07 (d, $J = 3.0$ Hz, 1H), 8.76 (d, $J = 12.0$ Hz, 1H), 8.71 (d, $J = 6.0$ Hz, 1H), 8.58 (s, 2H), 8.53 (s, 1H), 7.59 (d, $J = 6.0$ Hz, 1H), 7.41 (t, $J = 9.0$ Hz, 1H), 7.32 (m, 1H), 7.17 (t, $J = 9.0$ Hz, 2H), 3.51 (s, 2H), 3.19 (d, $J = 6.0$ Hz, 2H), 2.84 (d, $J = 15.0$ Hz, 2H), 2.05 (m, 1H), 2.26 (t, $J = 12.0$ Hz, 2H), 1.68 (d, $J = 12.0$ Hz, 2H), 1.57 (s, 1H), 1.23 (t, $J = 10.5$ Hz, 3H), 0.88 (d, $J = 3.0$ Hz, 4H). ^{13}C NMR (125 MHz, DMSO- d_6) δ 173.38, 165.25, 165.12, 161.20 (d, $^1J_{C-F} = 244.2$ Hz), 153.26, 149.12, 144.40, 143.93, 143.85, 135.59, 131.89 (d, $^3J_{C-F} = 4.8$ Hz), 130.76, 129.32 (d, $^3J_{C-F} = 8.0$ Hz), 127.04, 125.40 (d, $^2J_{C-F} = 15.1$ Hz), 124.55 (d, $^4J_{C-F} = 3.4$ Hz), 117.35, 115.51 (d, $^2J_{C-F} = 22.1$ Hz), 111.97, 55.35, 53.24, 45.28, 35.98, 30.22, 14.70, 8.29. HRMS (ESI): (M + H) $^+$ calcd for C₂₉H₃₂FN₆O₃, 531.2514; found, 531.2518.

5-(2-(Cyclopropanecarboxamido)isonicotinamido)-N-((1-(3-fluorobenzyl)piperidin-4-yl)methyl)nicotinamide (10c). Compound **10c** (61%) was synthesized by a procedure similar to that used to prepare compound **9a** as a light yellow solid. ^1H NMR (300 MHz, DMSO- d_6) δ 11.05 (s, 1H), 10.84 (s, 1H), 9.04 (d, $J = 1.9$ Hz, 1H), 8.77 (s, 1H), 8.72 (d, $J = 5.2$ Hz, 1H), 8.56 (s, 2H), 8.53 (d, $J = 5.0$ Hz, 1H), 7.58 (d, $J = 4.9$ Hz, 1H), 7.35 (dd, $J = 14.1, 7.5$ Hz, 1H), 7.18–7.10 (m, 2H), 7.06 (t, $J = 8.3$ Hz, 1H), 3.20 (s, 2H), 3.18 (s, 2H), 2.81 (d, $J = 9.2$ Hz, 2H), 2.05 (m, 1H), 1.94 (s, 2H), 1.68 (d, $J = 11.6$ Hz, 2H), 1.58 (s, 1H), 1.28–1.19 (m, 2H), 0.85 (d, $J = 7.0$ Hz, 4H). ^{13}C NMR (125 MHz, DMSO- d_6) δ 173.38, 165.26, 165.13, 162.67 (d, $^1J_{C-F} = 243.5$ Hz), 153.26, 149.14, 144.42, 143.92, 143.85, 135.60, 130.76, 130.50, 130.43, 127.05, 125.10, 117.36, 115.55 (d, $^2J_{C-F} = 20.6$ Hz), 114.06 (d, $^2J_{C-F} = 20.4$ Hz), 111.97, 62.03, 53.32, 49.06, 45.28, 35.99, 30.17, 14.71, 8.30. HRMS (ESI): (M + H) $^+$ calcd for C₂₉H₃₂FN₆O₃, 531.2514; found, 531.2522.

5-(2-(Cyclopropanecarboxamido)isonicotinamido)-N-((1-(4-fluorobenzyl)piperidin-4-yl)methyl)nicotinamide (10d). Compound **10d** (60%) was synthesized by a procedure similar to that used to prepare compound **9a** as a light yellow solid. ^1H NMR (500 MHz, DMSO- d_6) δ 11.05 (s, 1H), 10.85 (s, 1H), 9.03 (d, $J = 3.0$ Hz, 1H), 8.77 (s, 1H), 8.75 (s, 1H), 8.58 (s, 1H), 8.55 (d, $J = 9.0$ Hz, 1H), 8.52 (s, 1H), 7.57 (d, $J = 3.0$ Hz, 1H), 7.43 (s, 2H), 7.22 (s, 2H), 3.34 (s, 2H), 3.20 (s, 2H), 3.17 (d, $J = 5.0$ Hz, 2H), 2.09–2.01 (m, 1H), 1.76 (s, 2H), 1.69 (s, 1H), 1.43–1.25 (m, 2H), 1.19 (m, 2H), 0.90–0.81 (m, 4H). ^{13}C NMR (125 MHz, DMSO- d_6) δ 173.42, 169.18, 162.30 (d, $^1J_{C-F} = 239.8$ Hz), 153.28, 149.51, 149.20, 149.08, 144.49, 143.88, 143.81, 135.62 (d, $^2J_{C-F} = 24.6$ Hz), 130.69, 127.03, 125.97, 117.28, 115.79 (d, $^3J_{C-F} = 9.2$ Hz), 112.04, 49.13, 46.20, 29.48, 26.41, 14.68, 8.29. HRMS (ESI): (M + H) $^+$ calcd for C₂₉H₃₂FN₆O₃, 531.2514; found, 531.2519.

5-(2-(Cyclopropanecarboxamido)isonicotinamido)-N-((1-(3,4-difluorobenzyl) piperidin-4-yl)methyl)nicotinamide (10e). Compound **10e** (61%) was synthesized by a procedure similar to that used to prepare compound **9a** as a light yellow solid. ^1H NMR (300 MHz, DMSO- d_6) δ 11.05 (s, 1H), 10.84 (s, 1H), 9.05 (s, 1H), 8.77 (s, 2H), 8.56 (m, 2H), 8.53 (d, $J = 3.0$ Hz, 1H), 7.59 (d, $J = 3.0$ Hz, 1H),

7.13 (t, $J = 7.5$ Hz, 2H), 7.06 (t, $J = 4.5$ Hz, 1H), 3.51 (s, 2H), 3.18 (s, 2H), 2.84 (d, $J = 6.0$ Hz, 2H), 2.05 (m, 2H), 1.94 (s, 1H), 1.68 (d, $J = 9.0$ Hz, 2H), 1.58 (s, 1H), 1.23 (t, $J = 4.5$ Hz, 2H), 0.85 (d, $J = 6.0$ Hz, 4H). ^{13}C NMR (125 MHz, DMSO- d_6) δ 173.37, 165.25, 165.13, 158.33 (d, $^2J_{\text{C-F}} = 30.9$ Hz), 153.26, 150.69 (d, $^3J_{\text{C-F}} = 12.6$ Hz), 149.12, 144.45, 143.90, 135.61, 130.73, 127.05, 125.85, 118.96, 117.85 (dd, $^2,3J_{\text{C-F}} = 21.7, 8.1$ Hz), 117.54 (d, $^3J_{\text{C-F}} = 16.9$ Hz), 117.37, 116.57, 112.00, 61.23, 53.11, 45.20, 35.86, 29.99, 14.69, 8.28. HRMS (ESI): (M + H) $^+$ calcd for $\text{C}_{29}\text{H}_{31}\text{F}_2\text{N}_6\text{O}_3$, 549.2420; found, 549.2424.

N-((1-(3-chlorobenzyl)piperidin-4-yl)methyl)-5-(2-(cyclopropanecarboxamido)isonicotinamido)nicotinamide (**10f**). Compound **10f** (68%) was synthesized by a procedure similar to that used to prepare compound **9a** as a light yellow solid. ^1H NMR (500 MHz, DMSO- d_6) δ 11.05 (s, 1H), 10.86 (s, 1H), 9.04 (d, $J = 2.2$ Hz, 1H), 8.77 (d, $J = 1.6$ Hz, 1H), 8.74 (d, $J = 5.2$ Hz, 1H), 8.56 (d, $J = 3.2$ Hz, 2H), 8.53 (d, $J = 5.1$ Hz, 1H), 7.58 (dd, $J = 5.0, 1.2$ Hz, 1H), 7.36 (dd, $J = 15.1, 7.6$ Hz, 3H), 7.30 (s, 1H), 3.55 (s, 2H), 3.19 (t, $J = 5.9$ Hz, 2H), 2.86 (s, 2H), 2.11–2.00 (m, 2H), 1.99 (s, 1H), 1.70 (d, $J = 11.3$ Hz, 2H), 1.61 (s, 1H), 1.26 (d, $J = 4.4$ Hz, 2H), 0.90–0.81 (m, 4H). ^{13}C NMR (125 MHz, DMSO- d_6) δ 173.4, 165.3, 165.2, 153.3, 149.1, 144.4, 143.9, 135.6, 134.2, 133.4, 130.7, 130.6, 129.3, 128.1, 127.0, 120.6, 118.0, 117.4, 112.0, 60.2, 53.1, 45.2, 21.2, 14.7, 14.5, 8.3. HRMS (ESI): (M + H) $^+$ calcd for $\text{C}_{29}\text{H}_{32}\text{ClN}_6\text{O}_3$, 547.2219; found, 547.2224.

5-(2-(Cyclopropanecarboxamido)isonicotinamido)-*N*-((1-(2-methylbenzyl)piperidin-4-yl)methyl)nicotinamide (**10g**). Compound **10g** (56%) was synthesized by a procedure similar to that used to prepare compound **9a** as a light yellow solid. ^1H NMR (500 MHz, DMSO- d_6) δ 11.05 (s, 1H), 10.84 (s, 1H), 9.04 (d, $J = 2.4$ Hz, 1H), 8.77 (d, $J = 1.8$ Hz, 1H), 8.71 (t, $J = 5.6$ Hz, 1H), 8.60–8.54 (m, 2H), 8.53 (d, $J = 5.1$ Hz, 1H), 7.58 (m, 1H), 7.23–7.18 (m, 1H), 7.14 (d, $J = 3.4$ Hz, 2H), 7.12 (d, $J = 3.8$ Hz, 1H), 3.19 (d, $J = 5.9$ Hz, 2H), 3.17 (s, 2H), 2.79 (d, $J = 11.0$ Hz, 2H), 2.30 (s, 3H), 2.05 (m, 1H), 1.94 (t, $J = 10.8$ Hz, 2H), 1.67 (d, $J = 12.3$ Hz, 2H), 1.62–1.55 (m, 1H), 1.18 (d, $J = 9.4$ Hz, 2H), 0.85 (d, $J = 7.8$ Hz, 4H). ^{13}C NMR (125 MHz, DMSO- d_6) δ 173.4, 165.3, 165.1, 153.3, 149.1, 144.4, 143.9, 143.8, 137.4, 135.6, 130.8, 130.5, 129.8, 127.2, 127.0, 125.8, 117.4, 112.0, 60.9, 53.6, 49.1, 45.3, 36.2, 30.4, 19.3, 14.7, 8.3. HRMS (ESI): (M + H) $^+$ calcd for $\text{C}_{30}\text{H}_{35}\text{N}_6\text{O}_3$, 527.2765; found, 527.2774.

5-(2-(Cyclopropanecarboxamido)isonicotinamido)-*N*-((1-(3-methylbenzyl)piperidin-4-yl)methyl)nicotinamide (**10h**). Compound **10h** (59%) was synthesized by a procedure similar to that used to prepare compound **9a** as a light yellow solid. ^1H NMR (500 MHz, DMSO- d_6) δ 11.06 (s, 1H), 10.88 (s, 1H), 9.02 (d, $J = 2.2$ Hz, 1H), 8.82 (s, 1H), 8.78 (s, 1H), 8.61 (s, 1H), 8.56 (s, 1H), 8.53 (d, $J = 5.1$ Hz, 1H), 7.61–7.54 (m, 1H), 7.38–7.33 (m, 1H), 7.32–7.23 (m, 3H), 4.22 (s, 2H), 3.51 (s, 2H), 3.21 (s, 2H), 2.91 (s, 2H), 2.34 (s, 3H), 2.05 (m, 1H), 1.88 (d, $J = 13.3$ Hz, 2H), 1.84–1.75 (m, 1H), 1.43 (d, $J = 9.9$ Hz, 2H), 0.86 (d, $J = 6.2$ Hz, 4H). ^{13}C NMR (125 MHz, DMSO- d_6) δ 173.4, 165.3, 158.6, 158.4, 153.3, 149.2, 144.5, 143.9, 138.6, 135.6, 132.2, 132.1, 130.6, 129.2, 127.0, 118.9, 117.3, 116.6, 112.0, 51.9, 46.2, 44.4, 21.4, 14.7, 9.0, 8.3, 7.9. HRMS (ESI): (M + H) $^+$ calcd for $\text{C}_{30}\text{H}_{35}\text{N}_6\text{O}_3$, 527.2765; found, 527.2769.

5-(2-(Cyclopropanecarboxamido)isonicotinamido)-*N*-((1-(3-methoxybenzyl)piperidin-4-yl)methyl)nicotinamide (**10i**). Compound **10i** (47%) was synthesized by a procedure similar to that used to prepare compound **9a** as a light yellow solid. ^1H NMR (300 MHz, DMSO- d_6) δ 11.06 (s, 1H), 10.88 (s, 1H), 9.02 (s, 1H), 8.82 (s, 1H), 8.78 (s, 1H), 8.61 (s, 2H), 8.53 (d, $J = 3.0$ Hz, 1H), 7.59 (d, $J = 3.0$ Hz, 1H), 7.35 (t, $J = 4.5$ Hz, 1H), 7.28 (t, $J = 6.0$ Hz, 3H), 3.19 (s, 2H), 3.18 (m, 2H), 2.80 (s, 2H), 2.30 (s, 3H), 2.05 (t, $J = 4.5$ Hz, 1H), 1.93 (s, 2H), 1.67 (q, $J = 6.0$ Hz, 2H), 1.59 (s, 1H), 1.19 (m, 2H), 0.86 (d, $J = 3.0$ Hz, 4H). ^{13}C NMR (75 MHz, DMSO- d_6) δ 173.4, 165.3, 165.1, 159.7, 153.3, 149.2, 144.4, 144.0, 143.9, 135.6, 130.7, 129.6, 127.0, 121.4, 117.4, 114.6, 112.7, 112.1, 112.0, 62.7, 55.4, 53.4, 45.3, 36.0, 30.2, 14.7, 8.3. HRMS (ESI): (M + H) $^+$ calcd for $\text{C}_{30}\text{H}_{35}\text{N}_6\text{O}_4$, 543.2714;

found, 543.2716.

N-(1-(benzylpiperidin-4-yl)-5-(2-(cyclopropanecarboxamido)isonicotinamido)nicotinamide (**10j**). Compound **10j** (63%) was synthesized by a procedure similar to that used to prepare compound **9a** as a light yellow solid. ^1H NMR (500 MHz, DMSO- d_6) δ 11.02 (s, 1H), 10.90 (s, 1H), 9.02 (d, $J = 5.0$ Hz, 1H), 8.76 (s, 1H), 8.71 (d, $J = 7.3$ Hz, 1H), 8.55 (s, 1H), 8.52 (s, 1H), 8.51 (d, $J = 5.1$ Hz, 1H), 7.56 (d, $J = 5.1$ Hz, 1H), 7.48–7.39 (m, 5H), 4.04 (s, 2H), 3.21 (d, $J = 11.5$ Hz, 2H), 3.14 (t, $J = 7.2$ Hz, 1H), 2.82 (d, $J = 20.3$ Hz, 2H), 2.02 (d, $J = 6.1$ Hz, 1H), 2.00–1.94 (m, 2H), 1.78 (t, $J = 12.5$ Hz, 2H), 0.85 (d, $J = 5.5$ Hz, 4H). ^{13}C NMR (125 MHz, DMSO- d_6) δ 173.6, 165.4, 165.0, 153.1, 150.5, 149.2, 144.6, 144.0, 143.8, 135.5, 131.0, 130.6, 129.5, 129.1, 127.2, 117.4, 112.0, 56.5, 49.0, 46.3, 29.4, 14.7, 8.3. HRMS (ESI): (M + H) $^+$ calcd for $\text{C}_{28}\text{H}_{31}\text{N}_6\text{O}_3$, 499.3452; found, 499.2460.

N-(1-(3-chlorobenzyl)piperidin-4-yl)-5-(2-(cyclopropanecarboxamido)isonicotinamido)nicotinamide (**10k**). Compound **10k** (67%) was synthesized by a procedure similar to that used to prepare compound **9a** as a light yellow solid. ^1H NMR (500 MHz, DMSO- d_6) δ 11.05 (s, 1H), 10.88 (s, 1H), 9.04 (d, $J = 2.4$ Hz, 1H), 8.78 (s, 1H), 8.57 (d, $J = 2.3$ Hz, 1H), 8.56 (d, $J = 4.4$ Hz, 1H), 8.53 (d, $J = 5.1$ Hz, 1H), 7.63 (d, $J = 9.1$ Hz, 1H), 7.60–7.57 (m, 1H), 7.54 (d, $J = 7.6$ Hz, 1H), 7.49 (s, 3H), 4.13 (s, 2H), 3.20 (t, $J = 7.2$ Hz, 2H), 3.17 (s, 2H), 3.10 (d, $J = 7.5$ Hz, 2H), 2.05 (m, 2H), 1.76 (s, 2H), 0.91–0.81 (m, 4H). ^{13}C NMR (125 MHz, DMSO- d_6) δ 173.4, 165.3, 158.2, 153.2, 149.1, 144.6, 144.5, 144.0, 143.8, 135.6, 133.6, 132.7, 131.8, 131.7, 131.0, 131.0, 130.6, 127.1, 117.3, 111.9, 49.0, 46.2, 14.7, 9.0, 7.9. HRMS (ESI): (M + H) $^+$ calcd for $\text{C}_{28}\text{H}_{30}\text{ClN}_6\text{O}_3$, 533.2062; found, 533.2074.

N-(2-(1-(3-chlorobenzyl)piperidin-4-yl)ethyl)-5-(2-(cyclopropanecarboxamido)isonicotinamido)nicotinamide (**10l**). Compound **10l** (65%) was synthesized by a procedure similar to that used to prepare compound **9a** as a light yellow solid. ^1H NMR (300 MHz, DMSO- d_6) δ 11.07 (s, 1H), 10.86 (s, 1H), 9.04 (d, $J = 2.4$ Hz, 1H), 8.76 (d, $J = 1.6$ Hz, 1H), 8.68 (t, $J = 5.3$ Hz, 1H), 8.57 (s, 2H), 8.53 (d, $J = 5.1$ Hz, 1H), 7.58 (d, $J = 5.1$ Hz, 1H), 7.35 (t, $J = 7.6$ Hz, 2H), 7.30 (d, $J = 8.0$ Hz, 1H), 7.26 (d, $J = 7.2$ Hz, 1H), 3.45 (s, 2H), 3.32 (d, $J = 6.8$ Hz, 2H), 3.17 (d, $J = 4.9$ Hz, 2H), 2.78 (d, $J = 8.6$ Hz, 2H), 2.10–2.02 (m, 1H), 1.92 (d, $J = 4.3$ Hz, 1H), 1.69 (d, $J = 11.6$ Hz, 2H), 1.52–1.44 (m, 2H), 1.17 (m, 2H), 0.88–0.82 (m, 4H); ^{13}C NMR (75 MHz, DMSO- d_6) δ 173.4, 165.3, 164.8, 153.3, 149.2, 144.4, 143.9, 143.8, 141.9, 135.6, 133.3, 130.7, 130.5, 128.8, 127.8, 127.2, 127.0, 117.4, 112.0, 62.1, 53.7, 37.4, 36.2, 33.3, 32.3, 14.7, 8.3. HRMS (ESI): (M + H) $^+$ calcd for $\text{C}_{30}\text{H}_{34}\text{ClN}_6\text{O}_3$, 561.2375; found, 561.2386.

4.3. General procedure for the synthesis of target compounds 11a–11j

Tert-butyl 4-(((5-bromopyridin-3-yl)oxy)methyl)piperidine-1-carboxylate (**28a**). To a solution of intermediate **26a** (5.22 g, 30 mmol) in DMF (90 mL) was added of K_2CO_3 (10 g, 72 mmol) and intermediate **27a** (9.17 g, 33 mmol). The reaction mixture was stirred at 60 °C for 10 h. When TLC showed the completion of the reaction, the reaction mixture was cooled to room temperature and filtered off. The filtrate was evaporated off to dryness to give off-white intermediate **28a**, which could also be purified by recrystallization with MeOH as a white powder (70%). ^1H NMR (300 MHz, DMSO- d_6) δ 8.30–8.28 (m, 2H), 7.72 (t, $J = 2.1$ Hz, 1H), 3.97 (m, 2H), 3.94 (m, 2H), 2.74 (br s, 2H), 1.97–1.90 (m, 1H), 1.74 (d, $J = 12.0$ Hz, 2H), 1.40 (s, 9H), 1.21–1.08 (m, 2H). MS (ESI) m/z : 370.1 [M – H] $^-$.

Tert-butyl 4-(((5-bromopyridin-3-yl)oxy)methyl)piperidine-1-carboxylate (**28b**). To a solution of intermediate **26a** (1.73 g, 10 mmol) in DMF (20 mL) was added of K_2CO_3 (4.14 g, 30 mmol) and intermediate **27a** (3.96 g, 15 mmol). The reaction mixture was stirred at 60 °C for 10 h. When TLC showed the completion of the reaction, the reaction mixture was cooled to room temperature and filtered off. The filtrate was evaporated off to dryness to give off-white intermediate

28b, which could also be purified by recrystallization with MeOH as a white powder (53%). $^1\text{H NMR}$ (300 MHz, DMSO- d_6) δ 8.39 (d, $J = 2.5$ Hz, 1H), 8.36 (d, $J = 1.9$ Hz, 1H), 7.88 (t, $J = 2.2$ Hz, 1H), 4.79 (tt, $J = 8.0, 3.8$ Hz, 1H), 3.77 (t, $J = 5.0$ Hz, 1H), 3.73 (t, $J = 5.0$ Hz, 1H), 3.30–3.17 (m, 2H), 2.05–2.00 (m, 1H), 1.98 (dd, $J = 6.0, 3.4$ Hz, 1H), 1.60 (dd, $J = 11.8, 8.1, 3.5$ Hz, 1H), 1.48 (s, 9H).

Tert-butyl 4-((3-bromophenoxy)methyl)piperidine-1-carboxylate (28c). Intermediate **28c** was synthesized using the same method as that for **28b** by reacting **26 b** with **27a**. Light yellow solid (79%). $^1\text{H NMR}$ (300 MHz, DMSO- d_6) δ 7.25 (t, $J = 8.0$ Hz, 1H), 7.17–7.08 (m, 2H), 6.96 (dd, $J = 8.2, 2.4, 1.1$ Hz, 1H), 3.99 (d, $J = 13.1$ Hz, 2H), 3.86 (d, $J = 6.4$ Hz, 2H), 2.86–2.65 (m, 2H), 1.97–1.85 (m, 1H), 1.74 (dd, $J = 13.3, 3.4$ Hz, 2H), 1.42 (s, 9H), 1.15 (qd, $J = 12.4, 4.5$ Hz, 2H).

2-Acetamidoisonicotinic acid (22a). To a solution of compound **21** (3.04 g, 20 mmol) and K_2CO_3 (5.52 g, 40 mmol) in THF (100 mL) was slowly added acetyl chloride (2.8 mL, 40 mmol) wise over a period of 5 min in an ice bath. The mixture was allowed to stir at room temperature for 24 h. After complete reaction, K_2CO_3 was removed by filtration and methanol (30 mL) was added. After cooling, LiOH aqueous solution (12 mL, 3 mol/l) was added dropwise at 0 °C. The reaction solution was stirred at room temperature for 6 h. The organic solvent was removed and water (30 mL) was added. The pH of the solution was adjusted to 5 using 3 N HCl. The intermediate **22a** was filtered and dried as a white solid (67%). $^1\text{H NMR}$ (300 MHz, DMSO- d_6) δ 10.73 (s, 1H), 8.57 (s, 1H), 8.46 (dd, $J = 5.1, 0.7$ Hz, 1H), 7.50 (dd, $J = 5.1, 1.5$ Hz, 1H), 2.12 (s, 3H). *2-(Cyclopropanecarboxamido)isonicotinamide (29a)*. The carboxylic acid derivative **22** (1.65 g, 8.0 mmol) was dissolved in DMF (30 mL). DIPEA (3.97 mL, 24.0 mmol), HATU (3.95 g, 10.4 mmol) and ammonium chloride (4.24 g, 80.0 mmol) were added under ice-water bath conditions. The reaction solution was stirred at room temperature for 36 h. EA was added to the reaction solution and the precipitate was filtered. The filtrate was concentrated and purified by flash chromatography to give intermediate **29a** as a white powder (57%). $^1\text{H NMR}$ (300 MHz, DMSO- d_6) δ 10.90 (s, 1H), 8.42 (s, 1H), 8.40 (d, $J = 5.2$ Hz, 1H), 8.15 (s, 1H), 7.62 (s, 1H), 7.43 (dd, $J = 5.1, 1.5$ Hz, 1H), 0.83–0.81 (m, 4H). MS (ESI) m/z : 204.1 [M – H $^-$].

2-Acetamidoisonicotinamide (29b). Intermediate **29b** was synthesized using the same method as that for **29a** by reacting ammonium chloride with **22a**. Light yellow solid (63%). $^1\text{H NMR}$ (300 MHz, DMSO- d_6) δ 10.65 (s, 1H), 8.44 (s, 1H), 8.43 (d, $J = 5.4$ Hz, 1H), 8.23 (s, 1H), 7.70 (s, 1H), 7.47 (dd, $J = 5.1, 1.3$ Hz, 2H), 2.14 (s, 3H). MS (ESI) m/z : 178.1 [M – H $^-$].

Tert-butyl 4-(((5-(2-(cyclopropanecarboxamido)isonicotinamido)pyridin-3-yl)oxy)methyl)piperidine-1-carboxylate (30a). Intermediate **29a** (570 mg, 2.78 mmol), **28a** (1.14 g, 3.06 mmol), Pd2 (dba)₃ (128 mg, 0.14 mmol), xantphos (162 mg, 0.28 mmol) and Cs₂CO₃ (1.81 g, 5.56 mmol) was added to a dry schlenk tube. 1,4-dioxane (40 mL) was added under argon atmosphere. The reaction solution was stirred at 110 °C for 22 h. The reaction solution was filtered, and the filtrate was concentrated. The residue was resolved in EA, and the organic phase was washed with water (3 ×), 2 N aqueous HCl (1 ×), and brine (1 ×). After drying over MgSO₄ and filtration, the organic solvent was evaporated under reduced pressure. The solid was purified by flash chromatography to give intermediate **30a**. Light yellow powder (67%). $^1\text{H NMR}$ (300 MHz, DMSO- d_6) δ 11.09 (s, 1H), 10.72 (s, 1H), 8.56 (s, 1H), 8.53 (s, 1H), 8.10 (d, $J = 2.0$ Hz, 1H), 7.87 (m, 1H), 7.58–7.56 (m, 1H), 4.03–3.99 (m, 2H), 3.94 (d, $J = 6.0$ Hz, 2H), 2.76 (br s, 2H), 2.09–2.03 (m, 1H), 1.98 (br s, 1H), 1.79 (d, $J = 12.9$ Hz, 2H), 1.43 (s, 9H), 1.26–1.17 (m, 2H), 0.88 (d, $J = 6.1$ Hz, 4H). MS (ESI) m/z : 494.1 [M – H $^-$].

Tert-butyl 4-(((5-(2-(cyclopropanecarboxamido)isonicotinamido)pyridin-3-yl)oxy)methyl)piperidine-1-carboxylate (30b). Intermediate **30b** was synthesized using the same method as that for **30a** by reacting **29a** with **28b**. Light yellow solid (49%). $^1\text{H NMR}$ (300 MHz,

DMSO- d_6) δ 11.08 (s, 1H), 10.73 (s, 1H), 8.57 (d, $J = 2.0$ Hz, 2H), 8.54 (d, $J = 5.2$ Hz, 1H), 8.14 (d, $J = 2.6$ Hz, 1H), 7.89 (t, $J = 2.3$ Hz, 1H), 7.57 (dd, $J = 5.1, 1.6$ Hz, 1H), 4.64 (dp, $J = 12.1, 4.0$ Hz, 1H), 3.68 (t, $J = 7.1$ Hz, 2H), 3.26–3.21 (d, $J = 4.5$ Hz, 2H), 2.12–2.03 (m, 1H), 1.97–1.93 (m, 2H), 1.63–1.53 (m, 2H), 1.43 (d, $J = 1.4$ Hz, 9H), 0.90–0.81 (m, 4H). MS (ESI) m/z : 480.2 [M – H $^-$].

Tert-butyl 4-(((5-(2-(acetamidoisonicotinamido)pyridin-3-yl)oxy)methyl)piperidine-1-carboxylate (30c). Intermediate **30c** was synthesized using the same method as that for **30c** by reacting **29b** with **28a**. Light yellow solid (68%). $^1\text{H NMR}$ (300 MHz, DMSO- d_6) δ 10.77 (s, 1H), 10.72 (s, 1H), 8.56 (s, 1H), 8.54 (d, $J = 4.6$ Hz, 1H), 8.11 (d, $J = 2.7$ Hz, 1H), 7.89 (s, 1H), 7.58 (d, $J = 5.3$ Hz, 1H), 4.00 (d, $J = 12.9$ Hz, 2H), 3.95 (d, $J = 6.2$ Hz, 2H), 2.76 (br s, 2H), 2.16 (s, 3H), 2.04–1.94 (m, 1H), 1.78 (d, $J = 11.2$ Hz, 2H), 1.42 (s, 9H), 1.26–1.11 (m, 2H). MS (ESI) m/z : 468.2 [M – H $^-$].

Tert-butyl 4-(((3-(2-(acetamidoisonicotinamido)phenoxy)methyl)piperidine-1-carboxylate (30d). Intermediate **30d** was synthesized using the same method as that for **30a** by reacting **29a** with **28c**. Light yellow solid (60%). $^1\text{H NMR}$ (300 MHz, DMSO- d_6) δ 11.05 (s, 1H), 10.48 (s, 1H), 8.52 (s, 1H), 8.50 (d, $J = 5.3$ Hz, 1H), 7.54 (dd, $J = 4.9, 1.6$ Hz, 1H), 7.46 (t, $J = 2.2$ Hz, 1H), 7.36 (d, $J = 8.3$ Hz, 1H), 7.28 (t, $J = 8.1$ Hz, 1H), 6.73 (dd, $J = 7.8, 2.4$ Hz, 1H), 4.01 (d, $J = 13.0$ Hz, 2H), 3.85 (d, $J = 6.3$ Hz, 2H), 2.76 (br s, 2H), 2.11–2.03 (m, 1H), 2.01–1.89 (m, 1H), 1.78 (dd, $J = 13.2, 3.6$ Hz, 2H), 1.42 (s, 9H), 1.18 (qd, $J = 12.4, 4.4$ Hz, 2H), 0.91–0.82 (m, 4H). MS (ESI) m/z : 493.2 [M – H $^-$].

Tert-butyl 4-(((3-(2-(cyclopropanecarboxamido)isonicotinamido)phenoxy)methyl)piperidine-1-carboxylate (30e). Intermediate **30e** was synthesized using the same method as that for **30a** by reacting **29b** with **28c**. Light yellow solid (53%). $^1\text{H NMR}$ (300 MHz, DMSO- d_6) δ 10.74 (s, 1H), 10.47 (s, 1H), 8.51 (d, $J = 4.2$ Hz, 2H), 7.56 (d, $J = 5.4$ Hz, 1H), 7.48 (s, 1H), 7.36 (d, $J = 8.7$ Hz, 1H), 7.08 (d, $J = 10.6$ Hz, 1H), 6.74 (d, $J = 8.1$ Hz, 1H), 4.01 (d, $J = 10.6$ Hz, 2H), 3.86 (d, $J = 6.3$ Hz, 2H), 2.83–2.69 (m, 2H), 2.02–1.92 (m, 1H), 1.79 (d, $J = 12.7$ Hz, 2H), 1.43 (s, 9H), 1.18 (dt, $J = 12.1, 6.1$ Hz, 2H). MS (ESI) m/z : 467.1 [M – H $^-$].

N-(5-((1-benzylpiperidin-4-yl)methoxy)pyridin-3-yl)-2-(cyclopropanecarboxamido)isonicotinamide (11a). Compound **11a** (63%) was synthesized by a procedure similar to that used to prepare compound **9a** as a light yellow solid. $^1\text{H NMR}$ (300 MHz, DMSO- d_6) δ 11.06 (s, 1H), 10.70 (s, 1H), 8.54 (s, 2H), 8.51 (d, $J = 5.1$ Hz, 1H), 8.07 (d, $J = 2.5$ Hz, 1H), 7.85 (d, $J = 2.9$ Hz, 1H), 7.55 (d, $J = 5.1$ Hz, 1H), 7.35–7.29 (m, 4H), 7.25 (d, $J = 6.9$ Hz, 1H), 3.90 (d, $J = 6.0$ Hz, 2H), 3.47 (s, 2H), 2.92–2.77 (m, 2H), 2.09–2.03 (m, 1H), 1.96 (s, 2H), 1.77 (s, 1H), 1.75 (d, $J = 12.5$ Hz, 2H), 1.40–1.26 (m, 2H), 0.91–0.79 (m, 4H); $^{13}\text{C NMR}$ (125 MHz, DMSO- d_6) δ 173.4, 165.2, 155.2, 153.2, 149.1, 144.2, 139.0, 136.4, 134.5, 133.5, 129.3, 128.6, 127.4, 117.3, 113.1, 111.9, 72.9, 62.9, 53.2, 35.7, 28.8, 14.7, 8.3. HRMS (ESI): (M + H) $^+$ calcd for C₂₈H₃₂N₅O₃, 486.2500; found, 486.2493.

2-(cyclopropanecarboxamido)-N-(5-((1-(2-fluorobenzyl)piperidin-4-yl)methoxy)pyridin-3-yl)isonicotinamide (11b). Compound **11b** (74%) was synthesized by a procedure similar to that used to prepare compound **9a** as a light yellow solid. $^1\text{H NMR}$ (300 MHz, DMSO- d_6) δ 11.11 (s, 1H), 10.73 (s, 1H), 8.56 (s, 2H), 8.54 (s, 1H), 8.10 (d, $J = 2.6$ Hz, 1H), 7.87 (s, 1H), 7.57 (dd, $J = 5.1, 1.6$ Hz, 1H), 7.44 (m, 1H), 7.35–7.30 (m, 2H), 7.15–7.22 (m, 1H), 3.91 (d, $J = 5.9$ Hz, 2H), 3.54 (s, 2H), 2.88 (d, $J = 11.7$ Hz, 2H), 2.09 (s, 1H), 2.06–1.99 (m, 2H), 1.79 (s, 1H), 1.77 (s, 2H), 1.36–1.24 (m, 2H), 0.87 (m, 4H); $^{13}\text{C NMR}$ (75 MHz, DMSO- d_6) δ 173.38, 165.24, 161.23 (d, $^1J_{\text{C-F}} = 244.5$ Hz), 155.16, 153.22, 149.10, 144.15, 136.41, 134.45, 133.51, 131.99 (d, $^3J_{\text{C-F}} = 4.6$ Hz), 129.43 (d, $^3J_{\text{C-F}} = 8.5$ Hz), 125.30 (d, $^2J_{\text{C-F}} = 14.7$ Hz), 124.60 (d, $^4J_{\text{C-F}} = 3.5$ Hz), 117.36, 115.57 (d, $^2J_{\text{C-F}} = 22.0$ Hz), 113.11, 111.93, 72.89, 55.33, 53.05, 35.63, 28.86, 14.71, 8.32. HRMS (ESI): (M + H) $^+$ calcd for C₂₈H₃₁FN₅O₃, 504.2405; found, 504.2404.

2-(cyclopropanecarboxamido)-N-(5-((1-(4-fluorobenzyl)

piperidin-4-yl)methoxy) pyridin-3-yl)isonicotinamide (**11c**). Compound **11c** (70%) was synthesized by a procedure similar to that used to prepare compound **9a** as a light yellow solid. ^1H NMR (300 MHz, DMSO- d_6) δ 11.09 (s, 1H), 10.72 (s, 1H), 8.56 (d, $J = 1.7$ Hz, 2H), 8.54 (d, $J = 5.1$ Hz, 1H), 8.09 (d, $J = 2.6$ Hz, 1H), 7.87 (t, $J = 2.3$ Hz, 1H), 7.57 (dd, $J = 5.2, 1.6$ Hz, 1H), 7.39–7.30 (m, 2H), 7.20–7.10 (m, 2H), 3.91 (d, $J = 5.9$ Hz, 2H), 3.46 (s, 2H), 2.85 (m, 2H), 2.13–2.03 (m, 1H), 2.03–1.90 (m, 2H), 1.80 (d, $J = 5.0$ Hz, 1H), 1.78–1.69 (m, 2H), 1.33 (m, 2H), 0.92–0.82 (m, 4H); ^{13}C NMR (75 MHz, DMSO- d_6) δ 173.38, 165.24, 161.66 (d, $^1J_{\text{C-F}} = 242.5$ Hz), 155.16, 153.23, 149.10, 144.14, 136.42, 135.14, 134.44, 133.50, 131.04 (d, $^3J_{\text{C-F}} = 7.9$ Hz), 117.35, 115.30 (d, $^2J_{\text{C-F}} = 21.0$ Hz), 113.10, 111.93, 72.90, 61.94, 53.09, 35.74, 28.87, 14.71, 8.32. HRMS (ESI): (M + H) $^+$ calcd for C₂₈H₃₁FN₅O₃, 504.2405; found, 504.2402.

N-(5-((1-(2-chlorobenzyl)piperidin-4-yl)methoxy)pyridin-3-yl)-2-(cyclopropanecarboxamido)isonicotinamide (**11d**). Compound **11d** (74%) was synthesized by a procedure similar to that used to prepare compound **9a** as a light yellow solid. ^1H NMR (300 MHz, DMSO- d_6) δ 11.10 (s, 1H), 10.72 (s, 1H), 8.56 (d, $J = 2.0$ Hz, 2H), 8.54 (d, $J = 5.2$ Hz, 1H), 8.10 (d, $J = 2.6$ Hz, 1H), 7.87 (t, $J = 2.3$ Hz, 1H), 7.57 (dd, $J = 5.1, 1.6$ Hz, 1H), 7.51 (m, 1H), 7.44 (m, 1H), 7.39–7.26 (m, 2H), 3.93 (d, $J = 5.9$ Hz, 2H), 3.57 (s, 2H), 2.89 (d, $J = 11.7$ Hz, 2H), 2.12 (s, 1H), 2.09–2.01 (m, 2H), 1.81 (s, 1H), 1.77 (s, 2H), 1.45–1.29 (m, 2H), 0.93–0.81 (m, 4H); ^{13}C NMR (75 MHz, DMSO- d_6) δ 173.4, 165.3, 155.2, 153.2, 149.1, 144.1, 136.4, 134.5, 133.7, 133.5, 131.3, 131.2, 129.7, 129.0, 127.5, 117.4, 113.1, 111.9, 72.9, 59.4, 53.3, 35.6, 28.9, 14.7, 8.3. HRMS (ESI): (M + H) $^+$ calcd for C₂₈H₃₁ClN₅O₃, 520.2110; found, 520.2109.

N-(5-((1-benzylpiperidin-4-yl)oxy)pyridin-3-yl)-2-(cyclopropanecarboxamido)isonicotinamide (**11e**). Compound **11e** (42%) was synthesized by a procedure similar to that used to prepare compound **9a** as a light yellow solid. ^1H NMR (300 MHz, DMSO- d_6) δ 11.05 (s, 1H), 10.66 (s, 1H), 8.52 (d, $J = 2.0$ Hz, 2H), 8.50 (m, 1H), 8.07 (d, $J = 2.0$ Hz, 1H), 7.82 (t, $J = 2.0$ Hz, 1H), 7.54 (dd, $J = 5.1, 1.6$ Hz, 1H), 7.35–7.31 (m, 4H), 7.29–7.22 (m, 1H), 4.44–4.40 (m, 1H), 3.49 (s, 2H), 2.68–2.66 (m, 2H), 2.25 (t, $J = 9.0$ Hz, 1H), 2.06–2.06 (m, 1H), 2.00–1.95 (m, 2H), 1.70–1.60 (m, 2H), 0.86–0.84 (m, 4H); ^{13}C NMR (75 MHz, DMSO- d_6) δ 173.0, 164.8, 153.2, 152.8, 148.7, 143.7, 138.4, 136.0, 134.3, 134.1, 128.8, 128.2, 126.9, 116.9, 114.0, 111.5, 73.2, 62.0, 50.0, 30.5, 14.3, 7.9. HRMS (ESI): (M + H) $^+$ calcd for C₂₇H₃₀N₅O₃, 472.2343; found, 472.2357.

2-acetamido-*N*-(5-((1-(4-fluorobenzyl)piperidin-4-yl)methoxy)pyridin-3-yl)isonicotinamide (**11f**). Compound **11f** (58%) was synthesized by a procedure similar to that used to prepare compound **9a** as a light yellow solid. ^1H NMR (300 MHz, DMSO- d_6) 10.77 (s, 1H), 10.75 (s, 1H), 8.52 (s, 3H), 8.10 (d, $J = 2.1$ Hz, 1H), 7.95 (s, 1H), 7.60 (s, 1H), 7.56 (d, $J = 5.4$ Hz, 2H), 7.33 (t, $J = 8.8$ Hz, 2H), 4.31 (d, $J = 2.3$ Hz, 2H), 3.97 (d, $J = 5.4$ Hz, 2H), 3.42 (d, $J = 11.3$ Hz, 2H), 3.05–2.93 (m, 2H), 2.14 (s, 3H), 2.00 (d, $J = 13.9$ Hz, 2H), 1.90 (d, $J = 5.3$ Hz, 1H), 1.63–1.51 (m, 2H). ^{13}C NMR (125 MHz, DMSO- d_6) δ 170.07, 165.35, 163.22 (d, $^1J_{\text{C-F}} = 246.6$ Hz), 155.01, 153.29, 149.12, 144.04, 136.54, 134.20 (d, $^3J_{\text{C-F}} = 8.7$ Hz), 134.16, 133.01, 126.48, 117.33, 116.24 (d, $^2J_{\text{C-F}} = 21.7$ Hz), 113.64, 111.88, 71.84, 58.84, 51.54, 33.46, 26.04, 24.40. HRMS (ESI): (M + H) $^+$ calcd for C₂₆H₂₉FN₅O₃, 478.2249; found, 478.2259.

N-(3-((1-benzylpiperidin-4-yl)methoxy)phenyl)-2-(cyclopropanecarboxamido)isonicotinamide (**11g**). Compound **11g** (70%) was synthesized by a procedure similar to that used to prepare compound **9a** as a light yellow solid. ^1H NMR (300 MHz, DMSO- d_6) δ 11.02 (s, 1H), 10.44 (s, 1H), 8.50 (s, 1H), 8.49 (d, $J = 5.5$ Hz, 1H), 7.52 (dd, $J = 5.1, 1.6$ Hz, 1H), 7.44 (t, $J = 1.2$ Hz, 1H), 7.35 (s, 1H), 7.32–7.29 (m, 4H), 7.24 (t, $J = 8.0$ Hz, 2H), 6.70 (dd, $J = 8.0, 2.4$ Hz, 1H), 3.81 (d, $J = 5.8$ Hz, 2H), 3.47 (s, 2H), 2.85 (d, $J = 11.0$ Hz, 2H), 2.09–2.05 (m, 1H), 1.97 (t, $J = 10.6$ Hz, 2H), 1.78–1.75 (m, 1H), 1.73–1.71 (m, 2H), 1.34–1.27 (m, 2H), 0.87–0.83 (m, 4H). ^{13}C NMR (75 MHz, DMSO- d_6)

δ 173.3, 164.8, 159.3, 153.1, 148.9, 144.8, 140.2, 129.9, 129.3, 129.2, 128.6, 127.3, 117.3, 113.0, 112.0, 110.7, 107.0, 72.5, 62.8, 53.2, 35.8, 29.0, 14.7, 8.3. HRMS (ESI): (M + H) $^+$ calcd for C₂₉H₃₃N₄O₃, 485.2547; found, 485.2564.

2-(cyclopropanecarboxamido)-*N*-(3-((1-(4-fluorobenzyl)piperidin-4-yl)methoxy) phenyl)isonicotinamide (**11h**). Compound **11h** (61%) was synthesized by a procedure similar to that used to prepare compound **9a** as a light yellow solid. ^1H NMR (300 MHz, DMSO- d_6) 11.06 (s, 1H), 10.47 (s, 1H), 8.52 (s, 1H), 8.51 (s, 1H), 7.54 (d, $J = 6.4$ Hz, 1H), 7.46 (s, 1H), 7.37 (d, $J = 5.7$ Hz, 1H), 7.35 (d, $J = 5.6$ Hz, 2H), 7.27 (t, $J = 8.1$ Hz, 1H), 7.17 (t, $J = 8.9$ Hz, 2H), 6.73 (d, $J = 7.9$ Hz, 1H), 3.84 (d, $J = 5.7$ Hz, 2H), 3.47 (s, 2H), 2.85 (d, $J = 11.5$ Hz, 2H), 2.11–2.04 (m, 1H), 1.98 (t, $J = 11.1$ Hz, 2H), 1.79 (s, 1H), 1.76 (s, 2H), 1.31 (dd, $J = 14.1, 11.7$ Hz, 2H), 0.88 (d, $J = 5.0$ Hz, 4H). ^{13}C NMR (125 MHz, DMSO- d_6) δ 173.33, 164.79, 161.64 (d, $^1J_{\text{C-F}} = 242.2$ Hz), 159.35, 153.16, 148.96, 144.79, 140.23, 131.02 (d, $^3J_{\text{C-F}} = 8.2$ Hz), 129.95, 129.16, 117.35, 115.29 (d, $^2J_{\text{C-F}} = 21.1$ Hz), 112.99, 111.96, 110.74, 107.02, 72.49, 61.97, 53.16, 35.82, 29.04, 14.71, 8.28. HRMS (ESI): (M + H) $^+$ calcd for C₂₉H₃₂FN₄O₃, 503.2453; found, 503.2475.

2-acetamido-*N*-(3-((1-benzylpiperidin-4-yl)methoxy)phenyl)isonicotinamide (**11i**). Compound **11i** (68%) was synthesized by a procedure similar to that used to prepare compound **9a** as a light yellow solid. ^1H NMR (300 MHz, DMSO- d_6) 10.71 (s, 1H), 10.44 (s, 1H), 8.48 (d, $J = 4.4$ Hz, 2H), 7.53 (d, $J = 6.1$ Hz, 1H), 7.36–7.32 (m, 1H), 7.31 (m, 4H), 7.28–7.22 (m, 1H), 6.71 (d, $J = 8.0$ Hz, 1H), 3.82 (d, $J = 5.7$ Hz, 2H), 3.49–3.44 (m, 2H), 2.87–2.83 (m, 2H), 2.13 (s, 3H), 1.99–1.95 (m, 2H), 1.77 (s, 1H), 1.74 (m, 2H), 1.37–1.33 (m, 2H). ^{13}C NMR (75 MHz, DMSO- d_6) δ 170.0, 164.8, 159.3, 153.2, 149.0, 144.7, 140.2, 130.0, 129.3, 128.8, 128.6, 127.3, 117.4, 113.0, 111.9, 110.8, 107.0, 72.5, 62.9, 53.2, 35.8, 29.0, 24.4. HRMS (ESI): (M + H) $^+$ calcd for C₂₇H₃₁N₄O₃, 459.2391; found, 459.2413.

2-acetamido-*N*-(3-((1-(4-fluorobenzyl)piperidin-4-yl)methoxy) phenyl) isonicotinamide (**11j**). Compound **11j** (52%) was synthesized by a procedure similar to that used to prepare compound **9a** as a light yellow solid. ^1H NMR (300 MHz, DMSO- d_6) δ 10.73 (s, 1H), 10.45 (s, 1H), 8.49 (d, $J = 3.9$ Hz, 2H), 7.56–7.51 (m, 1H), 7.45 (s, 1H), 7.36 (m, 1H), 7.34–7.31 (m, 2H), 7.25 (t, $J = 8.0$ Hz, 1H), 7.14 (t, $J = 8.7$ Hz, 3H), 6.71 (d, $J = 8.4$ Hz, 1H), 3.81 (d, $J = 5.8$ Hz, 2H), 3.44 (s, 2H), 2.82 (d, $J = 9.0$ Hz, 2H), 2.13 (s, 3H), 1.95 (t, $J = 11.2$ Hz, 2H), 1.77 (m, 1H), 1.75–1.70 (m, 2H), 1.32–1.27 (m, 2H). ^{13}C NMR (150 MHz, DMSO- d_6) δ 169.99, 164.78, 161.64 (d, $^1J_{\text{C-F}} = 242.7$ Hz), 159.36, 153.21, 148.96, 144.75, 140.23, 135.29, 131.01 (d, $^3J_{\text{C-F}} = 7.5$ Hz), 129.96, 117.37, 115.30 (d, $^2J_{\text{C-F}} = 21.0$ Hz), 112.99, 111.91, 110.78, 107.00, 72.47, 61.99, 53.18, 35.85, 29.06, 24.41. HRMS (ESI): (M + H) $^+$ calcd for C₂₇H₃₀FN₄O₃, 477.2296; found, 477.2313.

4.4. General procedure for the synthesis of target compounds 12a–12c

Methyl 5-(1H-pyrrolo[2,3-b]pyridine-4-carboxamido)nicotinate (**33**). The carboxylic acid derivative **31** (4.60 g, 28.4 mmol) was dissolved in DMF (80 mL). DIPEA (11.17 mL, 70.7 mmol), HATU (12.90 g, 34.0 mmol) and **32** (5.62 g, 36.9 mmol) were added under ice bath conditions. The reaction solution was stirred at room temperature for 24 h. EA was added to the reaction solution and the precipitate was filtered. The filtrate was concentrated and purified by flash chromatography to give intermediate **33** as a light yellow solid (52%). ^1H NMR (300 MHz, DMSO- d_6) δ 11.07 (s, 1H), 10.35 (s, 1H), 8.97 (d, $J = 2.4$ Hz, 1H), 8.82 (m, 1H), 8.39 (m, 1H), 8.38 (d, $J = 6.1$ Hz, 1H), 7.90 (t, $J = 2.3$ Hz, 1H), 7.55 (d, $J = 2.3$ Hz, 1H), 6.69 (d, $J = 2.1$ Hz, 1H), 3.88 (s, 3H). MS (ESI) *m/z*: 295.1 [M – H] $^-$.

5-(1H-pyrrolo[2,3-b]pyridine-4-carboxamido)nicotinic acid (**34**). Compound **33** (2.95 g, 10 mmol) was dissolved in THF/MeOH (3:1, v/v, 60 mL) solution, and NaOH aqueous solution (30 mL, 1 mol/l) was

added dropwise under ice bath conditions. The reaction solution was stirred at room temperature for 7 h. The organic solvent was removed and water (60 mL) was added. The pH of the solution was adjusted to 5 with 3 N HCl. The intermediate **34** was filtered and dried as a white solid (76%). ^1H NMR (500 MHz, DMSO- d_6) δ 12.00 (s, 1H), 10.87 (s, 1H), 9.16 (d, $J = 2.4$ Hz, 1H), 8.83–8.81 (m, 2H), 8.41 (d, $J = 6.0$ Hz, 1H), 7.66 (t, $J = 3.0$ Hz, 1H), 7.58 (d, $J = 3.0$ Hz, 1H), 6.82 (d, $J = 2.1$ Hz, 1H). MS (ESI) m/z : 281.1 [M – H $^-$].

Tert-butyl 4-((5-(1H-pyrrolo[2,3-b]pyridine-4-carboxamido)nicotinamido)methyl) piperidine-1-carboxylate (35a). To a solution of **34** (1.40 g, 5.0 mmol) in THF (30 mL) was added DIPEA (2.48 mL, 15.0 mmol), followed by the addition of PyBOP (3.38 g, 6.5 mmol), HOBT (675 mg, 5 mmol) and 4-(aminomethyl)piperidine-1-carboxylic acid *tert* butyl ester (1.29 g, 6.0 mmol) under ice bath conditions. After stirring for 24 h at room temperature, the resulting mixture the resulting mixture was dropped into 100 mL of ice water, and extracted by EA. The organic phase was concentrated and purified by flash chromatography to give intermediate **35a** as a light yellow solid (69%). ^1H NMR (500 MHz, DMSO- d_6) δ 12.00 (s, 1H), 10.80 (s, 1H), 9.08 (d, $J = 2.0$ Hz, 1H), 8.78–8.77 (m, 1H), 8.66–8.65 (m, 1H), 8.57 (d, $J = 9.0$ Hz, 1H), 8.43 (d, $J = 2.0$ Hz, 1H), 7.68 (t, $J = 3.0$ Hz, 1H), 7.59 (d, $J = 3.0$ Hz, 1H), 6.85–6.83 (m, 1H), 3.96 (d, $J = 15.0$ Hz, 2H), 3.18 (d, $J = 2.0$ Hz, 2H), 2.89 (br s, 2H), 1.47 (m, 1H), 1.43 (s, 9H). MS (ESI) m/z : 477.1 [M – H $^-$].

Tert-butyl 4-(5-(1H-pyrrolo[2,3-b]pyridine-4-carboxamido)nicotinamido)piperidine-1-carboxylate (35b). Intermediate **35b** was synthesized using the same method as that for **35a** by reacting 4-amino-1-boc-piperidine with **34**. Light yellow solid (49%). ^1H NMR (s, 1H), 10.71 (s, 1H), 9.12 (d, $J = 2.1$ Hz, 1H), 8.69–8.64 (m, 1H), 8.60–8.55 (m, 1H), 8.18 (d, $J = 8.1$ Hz, 1H), 8.04 (d, $J = 2.1$ Hz, 1H), 7.59 (t, $J = 3.2$ Hz, 1H), 7.50 (d, $J = 3.2$ Hz, 1H), 6.81–6.77 (m, 1H), 3.29–3.20 (m, 1H), 3.21 (d, $J = 2.1$ Hz, 2H), 2.90 (br s, 2H), 1.51 (m, 1H), 1.43 (s, 9H). MS (ESI) m/z : 463.1 [M – H $^-$].

N-(5-(((1-(3-chlorobenzyl)piperidin-4-yl)methyl)carbamoyl)pyridin-3-yl)-1H-pyrrolo[2,3-b]pyridine-4-carboxamide (12a). Compound **12a** (59%) was synthesized by a procedure similar to that used to prepare compound **9a** as a light yellow solid. ^1H NMR (500 MHz, DMSO- d_6) δ 12.02 (s, 1H), 10.82 (s, 1H), 9.07 (d, $J = 2.4$ Hz, 1H), 8.77–8.75 (m, 2H), 8.66 (d, $J = 2.5$ Hz, 1H), 8.41 (d, $J = 4.9$ Hz, 1H), 7.67 (t, $J = 3.0$ Hz, 1H), 7.62 (s, 1H), 7.58 (d, $J = 4.9$ Hz, 1H), 7.36 (dd, $J = 14.9, 7.7$ Hz, 2H), 6.83 (t, $J = 2.5$ Hz, 1H), 3.51–3.49 (m, 2H), 3.21 (d, $J = 6.9$ Hz, 2H), 3.19–3.16 (m, 2H), 2.89–2.86 (m, 2H), 1.72–1.70 (m, 2H), 1.62 (s, 1H), 1.26–1.14 (m, 2H). ^{13}C NMR (100 MHz, DMSO- d_6) δ 166.3, 165.3, 150.1, 144.3, 143.6, 142.7, 135.9, 133.4, 133.3, 132.8, 131.3, 130.7, 130.6, 128.7, 126.8, 117.8, 114.0, 100.7, 59.2, 53.1, 52.7, 49.1, 7.9. HRMS (ESI): (M + H) $^+$ calcd for C₂₇H₂₈ClN₆O₂, 503.1957; found, 503.1942.

N-(5-(((1-benzylpiperidin-4-yl)carbamoyl)pyridin-3-yl)-1H-pyrrolo[2,3-b]pyridine-4-carboxamide (12b). Compound **12b** (68%) was synthesized by a procedure similar to that used to prepare compound **9a** as a light yellow solid. ^1H NMR (300 MHz, DMSO- d_6) δ 12.02 (s, 1H), 10.81 (s, 1H), 9.10 (d, $J = 2.4$ Hz, 1H), 8.78 (d, $J = 1.9$ Hz, 1H), 8.65 (t, $J = 2.1$ Hz, 1H), 8.58 (d, $J = 7.6$ Hz, 1H), 8.43 (d, $J = 4.9$ Hz, 1H), 7.69 (t, $J = 2.1$ Hz, 1H), 7.60 (d, $J = 5.0$ Hz, 1H), 7.39–7.35 (m, 4H), 7.32–7.26 (m, 1H), 6.85 (dd, $J = 3.4, 1.9$ Hz, 1H), 3.90–3.82 (m, 1H), 3.55 (s, 2H), 2.93–2.85 (m, 2H), 2.12 (m, 2H), 1.86 (d, $J = 10.8$ Hz, 2H), 1.64 (d, $J = 10.3$ Hz, 2H). ^{13}C NMR (75 MHz, DMSO- d_6) δ 166.3, 164.6, 150.2, 144.3, 143.7, 142.7, 135.9, 133.3, 130.8, 129.4, 128.7, 127.6, 126.8, 117.8, 114.0, 100.7, 62.3, 52.5, 47.3, 31.6, 14.4. HRMS (ESI): (M + H) $^+$ calcd for C₂₆H₂₇N₆O₂, 455.2190; found, 455.2199.

N-(5-(((1-(4-fluorobenzyl)piperidin-4-yl)carbamoyl)pyridin-3-yl)-1H-pyrrolo[2,3-b]pyridine-4-carboxamide (12c). Compound **12c** (66%) was synthesized by a procedure similar to that used to prepare compound **9a** as a light yellow solid. ^1H NMR (300 MHz, DMSO- d_6) δ 12.05 (s, 1H), 10.86 (s, 1H), 9.10 (s, 1H), 8.80 (s, 2H), 8.70

(s, 1H), 8.45 (d, $J = 4.7$ Hz, 1H), 7.70 (s, 1H), 7.67–7.59 (m, 3H), 7.37 (t, $J = 8.3$ Hz, 2H), 6.86 (s, 1H), 4.35 (s, 2H), 4.08 (s, 1H), 3.42 (s, 2H), 3.21–3.10 (m, 2H), 2.18–2.05 (m, 2H), 1.91–1.77 (m, 2H). ^{13}C NMR (100 MHz, DMSO- d_6) δ 166.38, 164.46, 158.17, 150.15, 144.48, 143.72, 142.72, 135.92, 134.25 (d, $^1J_{\text{C-F}} = 7.3$ Hz), 133.21, 130.47, 128.71, 126.77, 117.77, 116.27 (d, $^2J_{\text{C-F}} = 21.8$ Hz), 114.01, 100.63, 58.66, 51.13, 29.00, 7.92. HRMS (ESI): (M + H) $^+$ calcd for C₂₆H₂₆N₆O₂, 473.2096; found, 473.2090.

4.5. General procedure for the synthesis of target compound 12 d

1H-pyrrolo[2,3-b]pyridine-4-carboxamide (36). The carboxylic acid derivative **31** (1.62 g, 8.0 mmol) was dissolved in DMF (30 mL), DIPEA (3.97 mL, 24.0 mmol), HATU (3.95 g, 10.4 mmol) and ammonium chloride (4.24 g, 80.0 mmol) were added under ice-water bath conditions. The reaction solution was stirred at room temperature for 36 h. EA was added to the reaction solution and the precipitate was filtered. The filtrate was concentrated and purified by flash chromatography to give intermediate **36** as a white powder (63%). ^1H NMR (300 MHz, DMSO- d_6) δ 12.01 (s, 1H), 8.69 (m, 1H), 8.04–8.02 (m, 2H), 7.79 (br s, 1H), 7.51 (br s, 1H), 7.39 (s, 1H). MS (ESI) m/z : 160.1 [M – H $^-$].

Tert-butyl 4-(((5-(1H-pyrrolo[2,3-b]pyridine-4-carboxamido)pyridin-3-yl)oxy)methyl)piperidine-1-carboxylate (37). Intermediate **36** (448 mg, 2.78 mmol), **28a** (1.04 g, 2.78 mmol), Pd₂(dbc)₃ (128 mg, 0.14 mmol), xantphos (162 mg, 0.28 mmol) and Cs₂CO₃ (1.81 g, 5.56 mmol) was added to a dry schlenk tube. 1,4-dioxane (40 mL) was added under argon atmosphere. The reaction solution was stirred at 110 °C for 22 h. The reaction solution was filtered, and the filtrate was concentrated. The residue was resolved in EA, and the organic phase was washed with water (3 ×), 2 N aqueous HCl (1 ×), and brine (1 ×). After drying over MgSO₄ and filtration, the organic solvent was evaporated under reduced pressure. The solid was purified by flash chromatography to give intermediate **37**. Light yellow powder (52%). ^1H NMR (300 MHz, DMSO- d_6) δ 12.02 (s, 1H), 10.70 (s, 1H), 8.62 (d, $J = 2.0$ Hz, 1H), 8.41 (d, $J = 4.9$ Hz, 1H), 8.09 (d, $J = 2.0$ Hz, 1H), 7.96 (t, $J = 2.4$ Hz, 1H), 7.66 (d, $J = 2.1$ Hz, 1H), 7.58 (d, $J = 2.1$ Hz, 1H), 6.81 (d, $J = 2.1$ Hz, 1H), 4.02 (d, $J = 5.7$ Hz, 2H), 3.95 (d, $J = 6.0$ Hz, 2H), 2.75 (br s, 2H), 1.98 (br s, 1H), 1.80 (d, $J = 12.5$ Hz, 2H), 1.42 (s, 9H), 1.24–1.17 (m, 2H). MS (ESI) m/z : 450.1 [M – H $^-$].

N-(5-(((1-benzylpiperidin-4-yl)methoxy)pyridin-3-yl)-1H-pyrrolo[2,3-b]pyridine-4-carboxamide (12d). Compound **12d** (107 mg, 65%) was synthesized by a procedure similar to that used to prepare compound **9a** as a light yellow solid. ^1H NMR (300 MHz, DMSO- d_6) δ 12.03 (s, 1H), 10.70 (s, 1H), 8.61 (d, $J = 2.0$ Hz, 1H), 8.42 (d, $J = 4.9$ Hz, 1H), 8.10 (d, $J = 2.6$ Hz, 1H), 7.98 (t, $J = 2.4$ Hz, 1H), 7.72–7.64 (m, 1H), 7.57 (d, $J = 4.9$ Hz, 1H), 7.50–7.31 (m, 5H), 6.82 (m, 1H), 3.97 (d, $J = 5.7$ Hz, 2H), 3.87 (s, 2H), 3.20 (s, 2H), 3.13 (d, $J = 12.1$ Hz, 2H), 2.43 (s, 1H), 1.89 (d, $J = 12.5$ Hz, 2H), 1.51 (d, $J = 11.1$ Hz, 2H). ^{13}C NMR (75 MHz, DMSO- d_6) δ 166.0, 154.7, 149.7, 142.3, 136.4, 134.1, 133.1, 132.6, 128.5, 128.2, 117.4, 115.3, 113.6, 112.6, 100.2, 71.9, 52.0, 48.7, 28.5, 7.6. HRMS (ESI): (M + H) $^+$ calcd for C₂₆H₂₈N₅O₂, 442.2238; found, 442.2233.

4.6. Biology

In vitro AChE assay. The inhibitory activity of the target compounds against AChE was assessed by the Ellman method [31]. A stock solution of AChE was prepared by dissolving human recombinant AChE or electric eel AChE (Sigma Aldrich) lyophilized powder in 0.1 M phosphate buffer. Donepezil as positive control compound. Briefly, 40 μL of phosphate buffer (pH 8.0) was added to the 96-well plate, and then add different concentrations of the tested compounds (10 μL), AChE (10 mL, 2.5 U/mL), and DTNB (20 μL , 10 mM) at room temperature for 1 min. Then, 20 μL of

acetylthiocholine iodide (75 mM) was added to the reaction system. The plate was placed at 37 °C for 20 min, and then the absorbance was recorded at 415 nm using a microplate reader. Each concentration was analyzed in triplicate, and IC₅₀ of the compound were determined graphically from log concentration-inhibition curves (GraphPad Prism 8.0 software, GraphPad Software Inc.). Each IC₅₀ value was determined from at least two independent experiments each performed in triplicate.

GSK3β kinase assay. The GSK3β inhibitory activity of compounds was tested using Kinase-Glo assays method developed by Baki et al. [32] Recombinant human GSK3β (Merckmillipore) was assayed in buffer (50 mM HEPES (pH 7.5), 1 mM EDTA, 1 mM EGTA, and 15 mM magnesium acetate) using a GSK3 substrate peptide (GSM: RRRPASVPPSPSLS RHS(pS)HQRR) (Merckmillipore). Briefly, 10 μL of compound at different concentrations and GSK3β (10 μL, 20 ng) were added to the 96-well white plate, and then GSM peptide (10 μL, 25 μM) and ATP (10 μL, 1 μM) were added to each well. After a 30 min incubation at 30 °C, the enzymatic reaction was stopped with 40 μL of Kinase-Glo reagent (Promega). Each concentration was analyzed in triplicate, and the value of luminescence was recorded within 5 min using Molecular Devices ID5 multimode reader.

In vivo brain permeability and PK studies. All animal experiments were conducted in accordance with the relevant guidelines for animal containment and care, and all procedures were approved by the animal experiment ethics committee of the institution. The ICR mice were used in plasma-brain distribution assay of compounds. Mice were dosed with **11a** or **11c** (10 mg/kg p. o.). Blood samples and whole brain tissue were collected in EDTA coated tubes at t = 60 and 90 min after compound administration. Blood samples were centrifuged for 15 min at 5000 g at 4 °C. Brain homogenate samples were prepared by homogenizing the whole brain with 70% acetonitrile (1:2, w/v). An aliquot of plasma and brain (100 μL) was precipitated by addition of 20 μL internal standard and 280 μL of methanol solution containing 4 mM ammonium formate. After a quick centrifugation, the blood samples and brain homogenates were determined by LC/MS/MS using Hadera ODS-2 column (2.1 × 150 mm, 5 μm particles) with a flow rate of 1 mL/min. The LC-MS/MS system consisted of an Agilent 6224 series HPLC system (Agilent Technologies, USA) coupled to a Thermo TSQ mass spectrometer using positive-ion electrospray ionization (ESI) mode. The mobile phase consisted of water (containing 0.1% formic acid) (35%) and acetonitrile (65%). Compound **11e** was used as an internal standard. Mass to charge ratios (*m/z*) of 486.167 > 188.116, 504.165 > 206.103 and 472.160 > 174.120 were used for detection of **11a**, **11c** and **11e**, respectively.

The PK parameters were evaluated using non-compartmental analysis, based on the plasma concentration of the test compounds at different time points. Male SD rats (200–220 g, n = 6 per treatment group) were randomly assigned to treatment groups for the PK analysis. Compounds (**11a**, **11c**) dissolved in the vehicle (5% DMSO and 1% Tween 80 in saline) was administered to rats p. o. At 10 mg/kg or i. v. At 1 mg/kg. After administration, the blood samples were collected from the orbit into heparinized tubes at the designated time points (0.08, 0.25, 0.5, 1.0, 1.5, 3.0, 6.0, 8.0, 10.0, 12.0, and 24 h post-dosing for i. v.; 0.25, 0.5, 1.0, 2.0, 4.0, 8.0, 12.0, and 24 h post-dosing for p. o.). Blood samples (100 μL) were collected from the retro-orbital plexus into heparinized tubes and immediately centrifuged at 8000 rpm for 10 min to separate the plasma. Plasma samples were processed by protein precipitation with four volumes of MeOH and quantitative analyzed by LC-MS/MS as described above. The PK parameters were calculated according to a non-compartmental model using WinNonlin 8.0 (Certara).

In vivo AChE activity assay. Male ICR mice (25–30 g) were decapitated at 90 min after p. o. At 10 mg/kg administration of compounds (**11a**, **11c**, and donepezil). The brain samples were

weighed, and 20-fold the volume of buffer (10 mM HEPES, pH 7.5, 0.5% Triton X-100, 1 mM EGTA, 1 mM EDTA, and 150 mM NaCl) was added. The sample was homogenized and then centrifuged for 15 min at 3000 rpm at 4 °C. The protein concentration in the sample was quantified to 0.5 μg/mL using Enhanced BCA Protein Assay Kit (Beyotime). BChE activity was inhibited with ethopropazine hydrochloride (0.1 mM) for 5 min. The activity of AChE was assessed by the Ellman method as described above. The activity was determined by measuring the absorbance at 412 nm.

Detection of ACh in brain of ICR mice. LC-MS/MS was used to analyze ACh concentration in brain of ICR mice. Briefly, mice were decapitated at 90 min after p. o. At 10 mg/kg administration of compounds (**11a**, **11c**, and donepezil). Samples were weighed and homogenized in a 5-fold aliquot of H₂O. Brain homogenates (700 μL) were added to Eppendorf tubes containing acetonitrile (700 μL) for protein precipitation. The mixture was subsequently centrifuged at 5000 rpm for 10 min. The lower organic layer was transferred to a flask using a long needle syringe and evaporated to dryness under a gentle nitrogen stream. The residue was then solubilized in methanol (1 mL). Six identical MeOH-solubilized extracts of ACh were transferred into a single glass flask and evaporated to dryness under a gentle nitrogen stream. The residue was then solubilized in methanol (0.5 mL) and centrifuged at 12,000 rpm for 5 min. The LC-MS/MS system consisted of an Agilent 6224 series HPLC system (Agilent Technologies, USA) coupled to TSQ Quantum ULTRA AM mass spectrometer (Thermo) using positive-ion electrospray ionization (ESI) mode. Chromatography was performed on a Synchronis Amino column (250 × 2.1 mm, 5 μm, ThermoFisher) using mobile phase consisted of water (20%) and acetonitrile (80%) with a flow rate of 1 mL/min. Detection of positive ions was performed using the multiple reaction monitoring mode (MRM), the transition pair of ACh at the *m/z* 146.100 precursor ion to the *m/z* 86.905 product ion. The nominal concentration of ACh calibration standards in brain homogenate were 3.2, 12.5, 25, 50, 100 ng/mL. The calibration curve was linear over the concentration range 3.2–100 ng/mL of ACh in brain homogenate (Fig. S6).

5. Notes

The authors declare no competing financial interest.

Declaration of competing interest

The authors declare that they have no known competing financial interests or personal relationships that could have appeared to influence the work reported in this paper.

Acknowledgments

This work was supported by grant (No. 81973207) from National Natural Science Foundation of China and Natural Science Foundation of Jiangsu Province (No. BK20200571). We thank the support from “Double First-Class” initiative Innovation team project of China Pharmaceutical University (Nos. CPU2018GF10, CPU2018GY34).

Abbreviations

AD	Alzheimer's disease
AChE	acetylcholinesterase
ACh	acetylcholine
GSK3β	glycogen synthase kinase 3β
BBB	blood-brain-barrier
NMDA	N-methyl-D-aspartate
Aβ	amyloid-beta

MCA	UK Medicines Control Agency
NFTs	neurofibrillary tangles
CNS	central nervous system
BChE	butyrylcholinesterase
PAMPA	parallel artificial membrane permeability assay
SARs	structure-activity relationship
CAS	catalytic active site
PAS	peripheral anionic site
MD	molecular dynamics
LC/MS/MS	liquid chromatography with tandem mass spectrometry

Appendix A. Supplementary data

Supplementary data to this article can be found online at <https://doi.org/10.1016/j.ejmech.2021.113663>.

References

- [1] Alzheimer's Association Report, Alzheimer's disease facts and figures, *Alzheimer's Dement.* 2020 16 (3) (2020) 391–460.
- [2] H. Ashrafian, E.H. Zadeh, R.H. Khan, Review on Alzheimer's disease: inhibition of amyloid beta and tau tangle formation, *Int. J. Biol. Macromol.* 167 (2021) 382–394.
- [3] P.J. Whitehouse, D.L. Price, A.W. Clark, J. Coyle, M.R. DeLong, Alzheimer's disease: evidence for selective loss of cholinergic neurons in the nucleus basalis, *Ann. Neurol.* 10 (2) (1981) 115–126.
- [4] A.L. Decker, K. Duncan, Acetylcholine and the complex interdependence of memory and attention, *Curr Opin Behav Sci* 32 (2020) 21–28.
- [5] M.E. Hasselmo, The role of acetylcholine in learning and memory, *Curr. Opin. Neurobiol.* 16 (6) (2007) 710–715.
- [6] M. Bortolami, D. Rocco, A. Messori, R.D. Santo, F. Pandolfi, Acetylcholinesterase inhibitors for the treatment of Alzheimer's disease - a patent review (2016–present), *Expert Opin. Ther. Pat.* 19 (2021) 1–22.
- [7] Y. Zhou, Y. Fu, W.C. Yin, J. Li, W. Wang, F. Bai, S.T. Xu, Q. Gong, T. Peng, Y. Hong, D. Zhang, D. Zhang, Q. Liu, Y.C. Xu, H. Xu E, H.Y. Zhang, H.L. Jiang, H. Liu, Kinetics-driven drug design strategy for next-generation acetylcholinesterase inhibitors to clinical candidate, *J. Med. Chem.* 64 (2021) 1844–1855.
- [8] J.T. Brewster, S. Dell'Acqua, D.Q. Thach, J.L. Sessler, Classics in chemical neuroscience: donepezil, *ACS Chem. Neurosci.* 10 (2019) 155–167.
- [9] D.J. Selkoe, Alzheimer's disease is a synaptic failure, *Science* 298 (5594) (2002) 789–791.
- [10] M.T. Kabir, M.S. Uddin, A.A. Mamun, P. Jeandet, L. Aleya, R.A. Mansouri, G.M. Ashraf, B. Mathew, M.N. Binjumah, M.M. Abdeldaim, Combination drug therapy for the management of Alzheimer's disease, *Int. J. Mol. Sci.* 21 (9) (2020) 3272.
- [11] D. Peng, X. Yuan, R. Zhu, Memantine hydrochloride in the treatment of dementia subtypes, *J. Clin. Neurosci.* 20 (11) (2013) 1482–1485.
- [12] J.J. Miguel-Hidalgo, X.A. Alvarez, R. Cacabelos, G. Quack, Neuroprotection by memantine against neurodegeneration induced by β -amyloid (1–40), *Brain Res.* 958 (1) (2002) 210–221.
- [13] W.J. Deardorff, G. Grossberg, A fixed-dose combination of memantine extended-release and donepezil in the treatment of moderate-to-severe Alzheimer's disease, *Drug Des. Dev. Ther.* 10 (2016) 3267–3279.
- [14] O.L. Lopez, J.T. Becker, A.S. Wahed, J. Saxton, R.A. Sweet, D.A. Wolk, W. Klunk, S.T. Dekosky, Long-term effects of the concomitant use of memantine with cholinesterase inhibition in Alzheimer disease, *J. Neurol. Neurosurg. Psychiatry* 80 (6) (2009) 600–607.
- [15] A. Anighoro, J. Bajorath, G. Rastelli, Polypharmacology: challenges and opportunities in drug discovery, *J. Med. Chem.* 57 (19) (2014) 7874–7887.
- [16] L.Q. Zhu, S.H. Wang, D. Liu, Y.Y. Yin, Q. Tian, X.C. Wang, Q. Wang, J.G. Chen, J.Z. Wang, Activation of glycogen synthase kinase-3 inhibits long-term potentiation with synapse-associated impairments, *J. Neurol.* 27 (45) (2007) 12211–12220.
- [17] E. Lauretti, O. Dincer, D. Pratico, Glycogen synthase kinase-3 signaling in Alzheimer's disease, *Biochim. Biophys. Acta Mol. Cell Res.* 1867 (5) (2020) 118664.
- [18] L.Q. Zhu, S.H. Wang, D. Liu, Y.Y. Yin, Q. Tian, X.C. Wang, Q. Wang, J.G. Chen, J.Z. Wang, Activation of glycogen synthase kinase-3 inhibits long-term potentiation with synapse-associated impairments, *J. Neurol.* 27 (45) (2007) 12211–12220.
- [19] C.J. Yuskaitis, R.S. Jope, Glycogen synthase kinase-3 regulates microglial migration, inflammation, and inflammation-induced neurotoxicity, *Cell. Signal.* 21 (2) (2009) 264–273.
- [20] B. Eléonore, Regulation by glycogen synthase kinase-3 of inflammation and t cells in CNS diseases, *Front. Mol. Neurosci.* 4 (4) (2011) 18.
- [21] J.A. Morales-García, R. Luna-Medina, S. Alonso-Gil, M. Sanz-SanCristobal, V. Palomo, C. Gil, A. Santos, A. Martínez, A. Perez-Castillo, Glycogen synthase kinase 3 inhibition promotes adult hippocampal neurogenesis in vitro and in vivo, *ACS Chem. Neurosci.* 3 (11) (2012) 963–971.
- [22] X.Y. Jiang, J.T. Zhou, Y. Wang, X. Liu, K.Y. Xu, J. Xu, F. Feng, H.P. Sun, PROTACs suppression of GSK-3 β , a crucial kinase in neurodegenerative diseases [J], *Eur. J. Med. Chem.* 210 (2021) 112949.
- [23] O.V. Forlenza, V.J. De-Paula, B.S. Diniz, Neuroprotective effects of lithium: implications for the treatment of Alzheimer's disease and related neurodegenerative disorders, *ACS Chem. Neurosci.* 5 (2014) 443–450.
- [24] K. Oukoloff, N. Coquelle, M. Bartolini, M. Naldi, R.L. Guevel, S. Bach, B. Josselin, S. Ruchaud, M. Catto, L. Pisani, N. Denora, M.R. Iacobazzi, I. Silman, J.L. Sussman, F.E. Buron, J.P. Colletier, L. Jean, S. Routier, P.Y. Renard, Design, biological evaluation and X-ray crystallography of nanomolar multifunctional ligands targeting simultaneously acetylcholinesterase and glycogen synthase kinase-3, *Eur. J. Med. Chem.* 168 (2019) 58–77.
- [25] Jinyi Xu, Pengfei Zhang, Shengtao Xu, Zhanghai Yan, Qi Gong, Hong Yao, Shuai Qin, Renren Bai, Preparation Method and Application of Pyrimidinone Compound or its Pharmaceutically Salt. CN111349085, June30, 2020.
- [26] X.Y. Jiang, T.K. Chen, J.T. Zhou, S.Y. He, H.Y. Yang, Y. Chen, W. Qu, F. Feng, H.P. Sun, Dual GSK-3 beta/AChE inhibitors as a new strategy for multitargeting anti-Alzheimer's disease drug discovery, *ACS Med. Chem. Lett.* 9 (2018) 171–176.
- [27] X.Y. Jiang, J.T. Zhou, Y. Wang, L. Chen, Y. Duan, J.P. Huang, C. Liu, Y. Chen, W.Y. Liu, H.P. Sun, F. Feng, W. Qu, Rational design and biological evaluation of a new class of thiazolopyridyl tetrahydroacridines as cholinesterase and GSK-3 dual inhibitors for Alzheimer's disease, *Eur. J. Med. Chem.* 207 (2020) 112751.
- [28] X.Y. Jiang, Y. Wang, C. Liu, C.Y. Xing, Y.M. Wang, W.P. Lyu, S.S. Wang, Q.H. Li, T.K. Chen, Y. Chen, F. Feng, W.Y. Liu, H.P. Sun, Discovery of potent glycogen synthase kinase 3/cholinesterase inhibitors with neuroprotection as potential therapeutic agent for Alzheimer's disease, *Bioorg. Med. Chem.* 30 (2021) 115940.
- [29] G. Furlotti, M.A. Alisi, N. Cazzolla, P. Dragone, L. Durando, G. Magaro, F. Mancini, G. Mangano, R. Ombrato, M. Vitiello, A. Armirotti, V. Capurro, M. Lanfranco, G. Ottonello, M. Summa, A. Reggiani, Hit optimization of 5-substituted-n-(piperidin-4-ylmethyl)-1h-indazole-3-carboxamides: potent glycogen synthase kinase-3 (gsk-3) inhibitors with in vivo activity in model of mood disorders, *J. Med. Chem.* 58 (2015) 8920–8937.
- [30] G.L. Luo, L. Chen, C.R. Burton, et al., Discovery of isonicotinamides as highly selective, brain penetrable and orally active glycogen synthase kinase-3 inhibitors, *J. Med. Chem.* 59 (3) (2016) 1041–1051.
- [31] G.L. Ellman, K.D. Courtney, V. Andres, R.M. Featherstone, A new and rapid colorimetric determination of acetylcholinesterase activity, *Biochem. Pharmacol.* 7 (1961) 88–95.
- [32] A. Baki, A. Bielik, L. Molnár, G. Szendrei, G.M. Keserü, A high throughput luminescent assay for glycogen synthase kinase-3 beta inhibitor, *Assay Drug Dev. Technol.* 5 (2007) 75–83.
- [33] L.D. Pennington, D.T. Moustakas, The necessary nitrogen atom: a versatile high-impact design element for multi parameter optimization, *J. Med. Chem.* 60 (2017) 3552–3579.
- [34] Y. Zhou, J. Wang, Z. Gu, S. Wang, W. Zhu, J.L. Acena, V.A. Soloshonok, K. Izawa, H. Liu, Next generation of fluorine-containing pharmaceuticals, compounds currently in phase II-III clinical trials of major pharmaceutical companies: new structural trends and therapeutic areas, *Chem. Rev.* 116 (2016) 422–518.
- [35] M.M. Mesulam, C. Geula, Butyrylcholinesterase reactivity differentiates the amyloid plaques of aging from those of dementia, *Ann. Neurol.* 36 (2010) 722–727.
- [36] P. Bisignano, C. Lambruschini, M. Bicego, V. Murino, A.D. Favia, A. Cavalli, In silico deconstruction of atp-competitive inhibitors of glycogen synthase kinase-3 β , *J. Chem. Inf. Model.* 52 (2012) 3233–3244.
- [37] D. Choi, Glutamate neurotoxicity and diseases of the nervous system, *Neuron* 1 (1988) 623–634.
- [38] P. Oeckl, S. Halbgebauer, S. Anderl-Straub, C.A.F. Arnim, J. Diehl-Schmid, L. Froelich, T. Grimmer, L. Hausner, J. Denk, H. Jahn, P. Steinacker, H. Weishaupt Jh, A.C. Ludolph, M. Otto, Targeted mass spectrometry suggests beta-synuclein as synaptic blood marker in Alzheimer's disease, *J. Proteome Res.* 19 (2020) 1310–1318.
- [39] L. Reinhardt, S. Kordes, P. Reinhardt, M. Glatz, M. Baumann, H.C.A. Drexler, S. Menninger, G. Zischinsky, J. Eickhoff, C. Fro, P. Bhattarai, G. Arulmozhivarman, L. Marrone, A. Janosch, K. Adachi, M. Stettler, E.N. Anderson, M. Abo-Rady, M. Bickle, U.B. Pandey, M.M. Reimer, C. Kizil, H.R. Scholer, P. Nussbaumer, B. Klebl, J.L. Sternecker, Dual inhibition of gsk3 β and cdk 5 protects the cytoskeleton of neurons from neuroinflammatory-mediated degeneration in vitro and in vivo, *Stem Cell Rep* 12 (2019) 502–517.
- [40] A.J. Jalkanen, J.V. Leikas, M.M. Forsberg, Prolyl oligopeptidase inhibition decreases extracellular acetylcholine levels in rat hippocampus and prefrontal cortex, *Neurosci. Lett.* 579 (2014) 110–113.
- [41] I. Klinnenberg, A. Blokland, The validity of scopolamine as a pharmacological model for cognitive impairment: a review of animal behavioral studies, *Neurosci. Biobehav. Rev.* 34 (2010) 1307–1350.
- [42] I. Dolev, D.M. Michaelson, A nontransgenic mouse model shows inducible amyloid-beta (A β) peptide deposition and elucidates the role of apolipoprotein E in the amyloid cascade, *P Natl Acad Sci USA* 101 (2004) 13909–13914.